

Sodium Doping Effects on Properties of CZTS Thin Films
Fabricated by Sol-gel Convective Deposition Technique



A Thesis Submitted in Partial Fulfillment of the Requirements
for the Degree of Master of Engineering in Chemical Engineering

Department of Chemical Engineering

FACULTY OF ENGINEERING

Chulalongkorn University

Academic Year 2020

Copyright of Chulalongkorn University

ผลของการเจือโซเดียมต่อสมบัติของฟิล์มบางคอปเปอร์ซิงค์ทินซัลไฟด์
ที่สังเคราะห์ด้วยวิธีโซลเจลคอนเวคทีฟดีโพสิชัน



วิทยานิพนธ์นี้เป็นส่วนหนึ่งของการศึกษาตามหลักสูตรปริญญาวิศวกรรมศาสตรมหาบัณฑิต
สาขาวิชาวิศวกรรมเคมี ภาควิชาวิศวกรรมเคมี
คณะวิศวกรรมศาสตร์ จุฬาลงกรณ์มหาวิทยาลัย
ปีการศึกษา 2563
ลิขสิทธิ์ของจุฬาลงกรณ์มหาวิทยาลัย

Thesis Title	Sodium Doping Effects on Properties of CZTS Thin Films Fabricated by Sol-gel Convective Deposition Technique
By	Miss Orawan Sukchoy
Field of Study	Chemical Engineering
Thesis Advisor	Assistant Professor PARAVEE VAS-UMNUAY, Ph.D.
Thesis Co Advisor	Assistant Professor SOJIPHONG CHATRAPHORN, Ph.D.

Accepted by the FACULTY OF ENGINEERING, Chulalongkorn University in
Partial Fulfillment of the Requirement for the Master of Engineering

----- Dean of the FACULTY OF
ENGINEERING
(Professor SUPOT TEACHAVORASINSKUN, D.Eng.)

THESIS COMMITTEE

----- Chairman
(AKAWAT SRIRISUK, Ph.D.)

----- Thesis Advisor
(Assistant Professor PARAVEE VAS-UMNUAY, Ph.D.)

----- Thesis Co-Advisor
(Assistant Professor SOJIPHONG CHATRAPHORN, Ph.D.)

----- Examiner
(Assistant Professor Palang Bumroongsakulsawat, Ph.D.)

----- External Examiner
(Khomson Suttisintong, Ph.D.)

อรรวรรณ สุขช่วย : ผลของการเจือโซเดียมต่อสมบัติของฟิล์มบางคอปเปอร์ซิงค์ทินซัลไฟด์ที่สังเคราะห์ด้วยวิธีโซลเจลคอนเวคทีฟดีโพสิชัน. (Sodium Doping Effects on Properties of CZTS Thin Films Fabricated by Sol-gel Convective Deposition Technique) อ.ที่ปรึกษาหลัก : ผศ. ดร.ปารวี วาศน์อำนวย, อ.ที่ปรึกษาร่วม : ผศ. ดร. ไชยพงศ์ ฉัตรภรณ์

คอปเปอร์ซิงค์ทินซัลไฟด์ เป็นตัวเลือกหนึ่งที่น่าสนใจสำหรับการนำมาใช้ในเซลล์แสงอาทิตย์ชนิดฟิล์มบาง เนื่องจากประกอบด้วยสารที่หาได้ง่าย มีค่าช่องว่างแถบพลังงานที่เหมาะสม และมีค่าสัมประสิทธิ์การดูดกลืนแสงสูง อย่างไรก็ตามประสิทธิภาพของเซลล์แสงอาทิตย์ชนิดนี้ยังมีข้อจำกัด เนื่องจากมีข้อบกพร่องเชิงลบ เช่น ขนาดเกรนเล็ก มีรูพรุน ผิวฟิล์มไม่เรียบ และมีการแทนที่ของคอปเปอร์แทนซิงค์ ซึ่งทำให้ประสิทธิภาพของเซลล์แสงอาทิตย์ลดลง วิธีการที่มักใช้ในการเพิ่มประสิทธิภาพของเซลล์แสงอาทิตย์และลดข้อบกพร่องเชิงลบที่เกิดขึ้นคือการเจือด้วยโซเดียม ในงานนี้จึงทำการสังเคราะห์ฟิล์มบางคอปเปอร์ซิงค์ทินซัลไฟด์ด้วยวิธีโซลเจลคอนเวคทีฟดีโพสิชัน และเจือโซเดียมในฟิล์มโดยใช้ 2 วิธีคือ 1) เคลือบสารละลายโซเดียมคลอไรด์ความเข้มข้น 5 10 และ 15 มิลลิกรัมต่อมิลลิเมตรทึบบนฟิล์มคอปเปอร์ซิงค์ทินซัลไฟด์ และ 2) ผสมโซเดียมคลอไรด์ในสารละลายคอปเปอร์ซิงค์ทินซัลไฟด์ที่ความเข้มข้นร้อยละ 5 10 และ 15 ก่อนการขึ้นรูป ผลการวิจัยพบว่าการเจือโซเดียมในฟิล์มทั้งสองวิธี สามารถเพิ่มขนาดเกรน และทำให้ฟิล์มแน่นและเรียบมากขึ้น ฟิล์มที่ได้มีค่าช่องว่างแถบพลังงานอยู่ในช่วง 1.5 ถึง 1.6 อิเล็กตรอนโวลต์ และมีค่าสัมประสิทธิ์การดูดกลืนแสงสูง ซึ่งเหมาะกับการนำไปใช้ในเซลล์แสงอาทิตย์ การเจือโซเดียมในฟิล์มบางคอปเปอร์ซิงค์ทินซัลไฟด์ ยังทำให้ค่าแรงดันวงจรเปิด กระแสลัดวงจร พิลแพกเตอร์ และประสิทธิภาพของเซลล์แสงอาทิตย์เพิ่มขึ้น โดยประสิทธิภาพของเซลล์แสงอาทิตย์เพิ่มขึ้นจากร้อยละ 0.04 เป็นร้อยละ 0.18 เมื่อเจือโดยการเคลือบสารละลายโซเดียมคลอไรด์ 15 มิลลิกรัมต่อมิลลิเมตรทึบบนฟิล์มคอปเปอร์ซิงค์ทินซัลไฟด์

สาขาวิชา วิศวกรรมเคมี
ปีการศึกษา 2563

ลายมือชื่อนิสิต
ลายมือชื่อ อ.ที่ปรึกษาหลัก
ลายมือชื่อ อ.ที่ปรึกษาร่วม

6170328121 : MAJOR CHEMICAL ENGINEERING

KEYWORD: Thin-film solar cell, CZTS thin-film, Na-doping, Convective deposition
 Orawan Sukchoy : Sodium Doping Effects on Properties of CZTS Thin
 Films Fabricated by Sol-gel Convective Deposition Technique. Advisor: Asst.
 Prof. PARAVEE VAS-UMNUAY, Ph.D. Co-advisor: Asst. Prof. SOJIPHONG
 CHATRAPHORN, Ph.D.

$\text{Cu}_2\text{ZnSnS}_4$ (CZTS) is an interesting candidate for thin-film solar cell applications due to its availability and attractive properties (energy band gap of 1.5 eV and high absorption coefficient). However, CZTS solar cell performance is limited because of the defect formation from small grain size, pinholes, rough surface, and negative defects in CZTS such as Cu_{Zn} . One of the most possible ways to reduce these negative defects, and to increase solar cell performance is by doping with sodium. In this work, CZTS films were synthesized by sol-gel convective deposition technique and Na was doped in CZTS film using 2 different methods: 1) 5, 10, and 15 mg/ml of NaCl solutions were deposited on CZTS thin-film and 2) 5%, 10%, and 15% of NaCl were mixed with CZTS solution before deposited on a substrate. It was found from the results that Na-doped CZTS thin-films obtained from both methods could improve the grain size, enhance film compactness, reduce the grain boundaries and surface roughness. The energy band gap of the CZTS films was in range of 1.5-1.6 eV which was suitable for the solar cell application. Further investigation revealed that the V_{OC} , J_{SC} , and FF of Na-doped CZTS thin-film solar cells were improved accordingly, leading to better solar cell performance. The solar cell efficiency was increased from 0.04% (undoped CZTS thin-film) to 0.18% (15 mg/ml of NaCl solution doped on the CZTS-thin-film).

Field of Study: Chemical Engineering

Academic Year: 2020

Student's Signature

Advisor's Signature

Co-advisor's Signature

ACKNOWLEDGEMENTS

First of all, I would like to express my deep appreciation and gratitude to my thesis advisor, Asst. Prof. Dr. Paravee Vas-Umnuay and my co-advisor Asst. Prof. Dr. Sojiphong Chatraphorn for their guidance, suggestions, and assistance in this thesis. Without their supervision and assistance, this project would not have been completed.

Besides my advisor, I would like to thank the chairman and the committee members, Dr. Akawat Sirisuk, Asst. Prof. Dr. Palang Bumroongsukulsawad, and Dr. Khomson Suttisintong for their comments and useful suggestions on this thesis.

I respect and thank Miss Boonyaluk Namnuam for giving me all support and guidance that made me complete the project. I am extremely thankful to her for providing such nice support and guidance, although she had busy schedule managing.

In addition, I am thankful to members of the Center of Excellence in Particle Technology and Material Processing, Department of Chemical Engineering, Faculty of Engineering, Chulalongkorn University, and Semiconductor Physics Research Laboratory (SPRL), Department of Physics, Faculty of Science, Chulalongkorn University.

Finally, my achievement would never be possible unless there is hearty support from my family. The deepest and sincere gratitude goes to my beloved parents for their endless love, encouragement, and understanding throughout the entire period of my study.

จุฬาลงกรณ์มหาวิทยาลัย
CHULALONGKORN UNIVERSITY

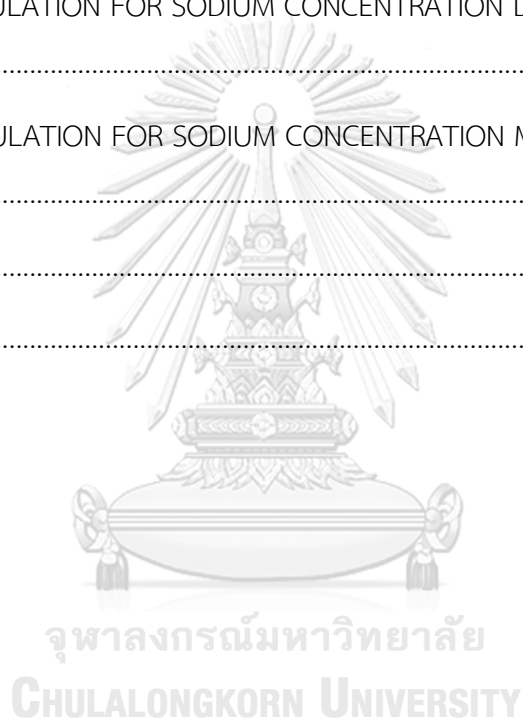
Orawan Sukchoy

TABLE OF CONTENTS

	Page
ABSTRACT (THAI)	iii
ABSTRACT (ENGLISH)	iv
ACKNOWLEDGEMENTS	v
TABLE OF CONTENTS	vi
LIST OF TABLES	ix
LIST OF FIGURES.....	x
CHAPTER 1 INTRODUCTION	1
1.1 Overview	1
1.2 Objectives	4
1.3 Scopes of Work.....	5
CHAPTER 2 FUNDAMENTAL THEORY AND LITERATURE REVIEWS	6
2.1 Solar Cells	6
2.2 Thin-Film Solar Cells	8
2.3 Copper Zinc Tin Sulfide.....	10
2.3.1 Copper Zinc Tin Sulfide Synthesis.....	10
2.3.2 Na-Doping in CZTS Thin-Film.....	13
2.3.3 CZTS synthesis using the Sol-gel Technique	16
2.3.4 Deposition Method for CZTS Solution	18
2.4 Convective Deposition Technique	21
2.5 CZTS Thin-Film Solar Cell Structure.....	23
2.6 Characteristics of Solar Cell.....	25

CHAPTER 3 EXPERIMENTAL.....	27
3.1 Synthesis of CZTS Thin-Films.....	27
3.1.1 Chemicals.....	28
3.1.2 Preparation of CZTS Precursor Solution.....	28
3.1.3 Preparation of Na-Doped CZTS Precursor Solution.....	28
3.1.4 Preparation of NaCl Solution.....	28
3.1.5 Deposition of CZTS Thin-Film.....	29
3.2 Fabrication of CZTS Thin-Film Solar Cell.....	29
3.2.1 SLG Substrate Preparation.....	30
3.2.2 Mo Deposition.....	30
3.2.3 CZTS Thin-Film Deposition.....	30
3.2.4 CdS Deposition.....	31
3.2.5 i-ZnO Deposition.....	31
3.2.6 ZnO(Al) Deposition.....	31
3.2.7 Al Grid.....	32
3.3 Analytical Instruments.....	32
3.3.1 X-ray Diffraction (XRD).....	32
3.3.2 Scanning Electron Microscope (SEM).....	32
3.3.3 Energy Dispersive X-ray Spectroscopy (EDS).....	32
3.3.4 Atomic Force Microscopy (AFM).....	32
3.3.5 UV-Visible Spectrophotometer.....	32
3.3.6 Current-Voltage Characteristics.....	33
CHAPTER 4 RESULTS AND DISCUSSION.....	34
4.1 Na-doping Effects on Structural Properties of CZTS Thin-Film.....	36

4.2 Na-doping Effects on Optical Properties of CZTS Thin-Film.....	47
4.3 Na-doping Effects on the Solar Cell Performance	49
CHAPTER 5 CONCLUSIONS AND RECOMMENDATIONS	54
5.1 Conclusions.....	54
5.2 Recommendations.....	54
APPENDIX A CALCULATION FOR CZTS SOL-GEL SOLUTION	56
APPENDIX B CALCULATION FOR SODIUM CONCENTRATION DEPOSITED ON THE CZTS THIN-FILM.....	57
APPENDIX C CALCULATION FOR SODIUM CONCENTRATION MIXED IN THE CZTS SOL- GEL SOLUTION	58
REFERENCES.....	59
VITA	65



LIST OF TABLES

	Page
Table 1: The amount of chemicals used in chemical bath deposition.....	31
Table 2: Na concentration on the CZTS thin-films.	34
Table 3: Chemical composition of undoped and Na-doped CZTS thin-films.....	37
Table 4: Element ratios of undoped and Na-doped CZTS thin-films.	37
Table 5: Lattice parameters and volume of unit cell estimated for the undoped and Na-doped CZTS film.....	40
Table 6: The corresponding XRD characteristics of (112) plane.	41
Table 7: Characteristics parameters of CZTS, CZTS/15, and CZTS+5 solar cells*.	52

LIST OF FIGURES

	Page
Figure 1: Schematic of thin-film solar cell structure.....	2
Figure 2: Different generations of solar cells [13-15].	7
Figure 3: Silicon solar cells [19].	7
Figure 4: Working principle of a solar cell [21].	9
Figure 5: Crystal structures of CZTS [23].	10
Figure 6: Thin-film deposition techniques.	11
Figure 7: SEM images of CZTS thin-films with 0 nm (a), 10 nm (b), and 20 nm (c) of NaF.	13
Figure 8: XRD patterns of CZTS thin-film doped with 0%, 10%, 20%, and 30% of Na.	14
Figure 9: SEM images of CZTS thin-films with 3.9%, 4.3%, 4.8%, and 5.4% Na-doping.	15
Figure 10: SEM images of the CZTSSe film (c, e) and 5 mg/ml Na-doped CZTSSe films (d, f).	16
Figure 11: Thin-film deposition using the sol-gel method [31].	17
Figure 12: Graphical representation of spin coating technique [33].	19
Figure 13: Graphical representation of dip-coating technique [31].	19
Figure 14: Graphical representation of spray coating techniques [34].	20
Figure 15: Graphical representation of doctor blade coating techniques [34].	20
Figure 16: Convective deposition technique.	22
Figure 17: Schematic of CZTS thin-film solar cell structure.	23
Figure 18: I-V and P-V characteristics of a typical solar cell [38].	25

Figure 19: Preparation of undoped and Na-doped CZTS thin-films.	27
Figure 20: Thin-film deposition using convective deposition technique.	29
Figure 21: Schematic of CZTS thin-film solar cell fabrication.	30
Figure 22: The XRD patterns of as-CZTS and annealed CZTS thin-films. The annealed films were performed in N ₂ atmosphere for 30 minutes. The film thickness is about 300 nm.	35
Figure 23: The XRD patterns of undoped and Na-doped CZTS thin-films. The films were annealed at 550°C in N ₂ atmosphere for 30 minutes. The film thickness is about 1.2 μm.	38
Figure 24: Top-view SEM images of undoped and Na-doped CZTS thin-films. The films were annealed at 550°C in N ₂ atmosphere for 30 minutes. The film thickness is about 1.2 μm.	43
Figure 25: Grains size distribution of undoped and Na-doped CZTS thin-films. The grains size was measured by the ImageJ program for 100 grains from 3 pictures.	44
Figure 26: Cross-sectional SEM images of CZTS (a, d), CZTS/15 (b, e), and CZTS+5 (c, f) films.	46
Figure 27: AFM images and height profiles of CZTS (a, d), CZTS/15 (b, e), and CZTS+5 (c, f) films.	47
Figure 28: Plot of absorption coefficient of undoped and Na-doped CZTS thin-films.	48
Figure 29: Tauc plot of $(\alpha h\nu)^2$ vs. photon energy ($h\nu$) of undoped and Na-doped CZTS thin-films. The dash line is extrapolated to determine energy band gap (E_g).	49
Figure 30: Photographs of CZTS thin-film on Mo coated SLG (a), SLG/Mo/CZTS/CdS (b), SLG/Mo/CZTS/CdS/i-ZnO (c), SLG/Mo/CZTS/CdS/i-ZnO/ZnO(Al) (d), SLG/Mo/CZTS/CdS/i-ZnO/ZnO(Al)/Al (e), CZTS thin-film solar cell (f).	50
Figure 31: The plot of solar cell parameters of CZTS, CZTS/15, and CZTS+5.	51
Figure 32: The J-V curves of CZTS, CZTS/15, and CZTS+5 thin-film solar cells.	52

CHAPTER 1

INTRODUCTION

1.1 Overview

At present, the demand for electricity is dramatically increased due to economic, industrial, and technology growth. Therefore, more electrical energy is generated to meet the needs of users. However, most of the electrical energy is produced from fossil fuels such as natural gas, petroleum, and coal which is gradually depleting in the near future. Moreover, the burning of fossil fuels emits carbon dioxide, which is one of the greenhouse gases that contributes to air pollution and global warming. Currently, researchers are increasingly interested in the developing of electricity generation from renewable energy sources especially solar energy, which is the cleanest and most abundant source of renewable energy. Solar energy can be converted into electrical energy by an electrical device called solar cells.

Thin-film solar cells are one of the most widely used solar cells because they have many advantages of high efficiency and durability, low material consumption, and low production cost. Manufacture of thin-film solar cells is performed by depositing a light-absorbing material onto a substrate, e.g. glass, plastic, and metal. In general, the light-absorbing materials are made of semiconductors which are very thin, thus thin-film solar cells are more flexible and light weight than other conventional solar cells.

Thin-film solar cells consist of substrate, back contact, absorber layer, buffer layer, window layer, transparent conducting oxide, and front contact, as shown in **Figure 1**.

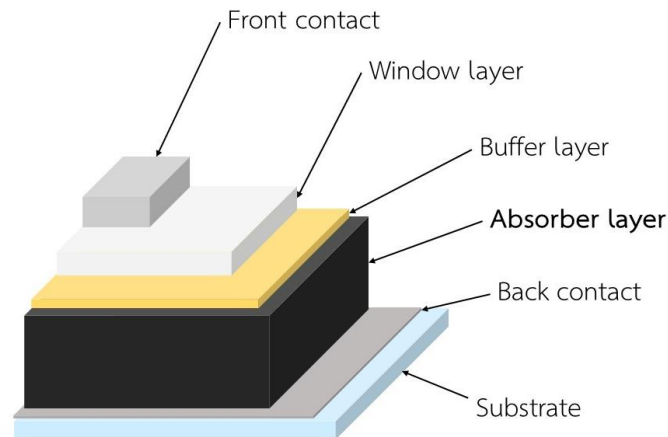


Figure 1: Schematic of thin-film solar cell structure.

In the thin-film solar cell, the layer that has a significant effect on solar cell efficiency is the absorber layer. This layer must be 1-2 μm thick to have enough volume to absorb the solar spectrum and generate electron-hole pairs. In addition, the absorber layer must have a large grain and dense film in order to achieve high efficiency of solar cell.

There are 3 main types of thin-film solar cells in the market, depending on the type of absorber layer used: amorphous silicon (a-Si), cadmium telluride (CdTe), and copper indium gallium selenide (CIGS). However, a-Si has a significant degradation in the power output when they are exposed to the sun. In addition, the material is not easy to find in the market. CdTe solar cell has high efficiency of 22.1% at laboratory scale [1]. Since cadmium is a highly toxic element, there are health concerns regarding the use of cadmium in thin-film solar cells. CIGS solar cell has the highest efficiency of 22.6% [2] but a large-scale production is limited because of the less availability of indium and gallium in earth crust. Therefore, the new quaternary material copper zinc tin sulfide ($\text{Cu}_2\text{ZnSnS}_4$; CZTS) which is composed of earth-abundant and non-toxic element, is the next best candidate to replace CIGS solar cells. CZTS has optimal energy band gap of around 1.5 eV and high absorption coefficient ($>10^4 \text{ cm}^{-1}$) [3] which is suitable to use as an absorber in thin-film solar cells.

The CZTS thin-film layer can be deposited by either physical processes such as sputtering, and co-evaporation methods or chemical processes such as sol-gel method. The physical processes are very effective method. However, it requires a vacuum environment, resulting in a high production cost. Whereas the sol-gel process is less expensive, which is more suitable for a large-scale production. The sol-gel solution can be deposited on a substrate to form CZTS thin-film using a general deposition technique such as spin coating, spray coating, dip coating, doctor blade coating [4], and convective deposition. In this thesis, the sol-gel convective deposition technique was used to synthesis the CZTS thin-film.

The convective deposition technique has many advantages over other techniques. It is a simple technique and does not require a vacuum environment. In addition, convective deposition has high-throughput production which is suitable for coating on large areas. Moreover, convective deposition requires just a few microliters of precursor solution to prepare a uniform film. The deposition process is started by injecting a precursor solution to the injection point (between the substrate and the deposition blade). Then the substrate is pulled horizontally to form a thin layer of solution on the substrate. As mentioned above, the thickness and characteristics of the CZTS film affect the efficiency of solar cells. Therefore, the parameters that affect the film such as the deposition speed, deposition temperature, pre-heating temperature, annealing temperature, and the precursor concentration must be properly controlled to achieve a uniform thin-film for use as an absorber layer in CZTS solar cell.

The suitable CZTS thin-film for use as an absorber layer in CZTS solar cells must be dense, smooth and has a large grain size in order to prevent the recombination of electrons and holes. However, the CZTS film synthesized by a solution-based process has some drawbacks. The CZTS thin-film may have a small grain size, pinholes, or cracks formation. Voids and cracks in the CZTS thin-film lead to low efficiency because the generated carriers recombine. One of the methods to enhance the grain size and the crystallinity of the CZTS thin-film is to increase annealing time and

temperature after the deposition process [4, 5], or by mixing the CZTS nanoparticles with CZTS precursor solution [6, 7] in order to form a smooth and dense film with larger grain size. In addition, there are several studies that attempted to improve the CZTS thin-film by doping with alkali metals such as lithium (Li), sodium (Na), potassium (K), and rubidium (Rb). Doping these metals into CIGS and CZTS thin-film have been proved to be positive effects such as promoting crystal growth, reducing point defects, reducing the secondary phase, increasing p-type carrier concentration, and passivating the grain boundaries [8-12]. The metal doping can be done both after thin-film deposition by depositing the metal solution onto the CZTS thin-film and during thin-film deposition by adding the metal in the CZTS precursor solution.

In this work, the CZTS thin-films were synthesized using the sol-gel convective deposition technique and the properties of the film were improved by doping with Na. The effects of Na doping concentration and doping methods were investigated in terms of structural and optical properties (grain size, crystal size, roughness surface, and optical band gap). Na-doping after thin-film deposition was expected to increase grain size and smooth CZTS thin-film, while Na-doping during the thin-film deposition was expected to increase crystal size, grain size, and uniform size CZTS thin-film.

1.2 Objectives

- 1.2.1 To synthesize CZTS thin-films by convective deposition method as an absorber layer in CZTS thin-film solar cell.
- 1.2.2 To investigate the effects of Na-doping in CZTS thin-films using 2 methods:
 - 1.2.2.1 A NaCl was mixed with CZTS solution and deposited on a substrate by convective deposition.
 - 1.2.2.2 A solution of NaCl was deposited on CZTS thin-films by convective deposition.

1.3 Scopes of Work

- 1.3.1 CZTS thin-films were synthesized in liquid phase by sol-gel convective deposition method.
 - 1.3.1.1 CZTS solution was synthesized using concentration of Cu:Zn:SnS equal to 0.48:0.31:0.25:2 M and 2-methoxyethanol was used as a solvent.
 - 1.3.1.2 30 microliters of CZTS solution were used to fabricated each layer of CZTS thin-film.
 - 1.3.1.3 Deposition speed of convective deposition was set to 500 $\mu\text{m/s}$
 - 1.3.1.4 CZTS thin-film was heated at 200°C for 10 minutes on a hotplate in air and annealed at 550°C for 30 minutes in nitrogen atmosphere.
 - 1.3.1.6 For Na-doping by mixing NaCl in CZTS solution, 5%, 10%, and 15% NaCl to CZTS molar ratio were added to the final CZTS solution and were used to fabricated CZTS thin-film.
 - 1.3.1.7 For Na-doping by depositing NaCl solution on CZTS film, NaCl solution with 5, 10, and 15 mg/ml in ethanol and DI water mixed solvent were used to deposited on CZTS thin-film.

CHAPTER 2

FUNDAMENTAL THEORY AND LITERATURE REVIEWS

2.1 Solar Cells

A solar cell, or photovoltaic cell, is an electrical device that catches the sunlight and turns it directly into electricity without any intermediate process. When the sunlight hits the semiconductor in solar cell, electrons are excited and started moving. The unidirectional movement of electrons produces electricity.

Solar cells are characterized in categories called generations which can be classified into 3 generations: 1st generation, 2nd generation, and 3rd generation. Generations of solar cells can be summarized in **Figure 2**.



First Generation

- Monocrystalline Silicon Cell
- Polycrystalline Silicon Cell
- Amorphous Silicon Cell



Second Generation

- Amorphous silicon (a-Si)
- Cadmium Telluride (CdTe)
- Copper Indium Gallium Selenide (CIGS)
- Copper Zinc Tin Sulfide (CZTS)

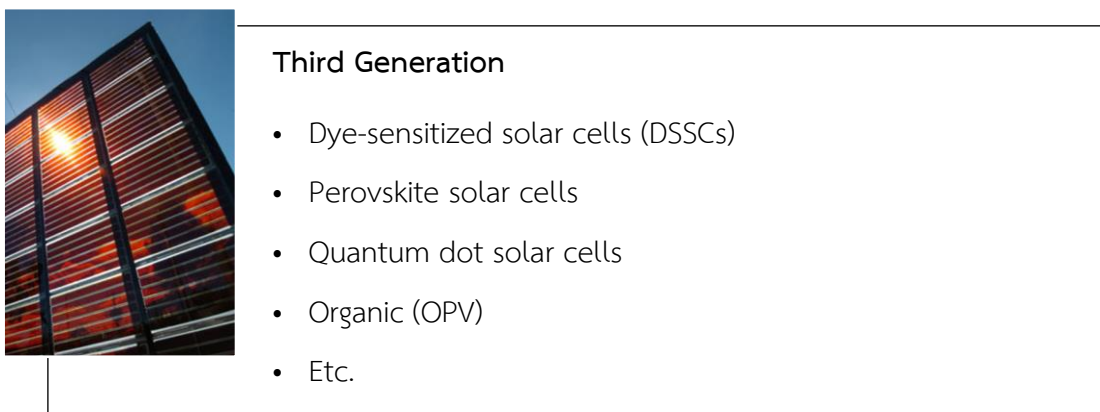


Figure 2: Different generations of solar cells [13-15].

First-generation solar cells are made of silicon wafers. There are 2 types of silicon used in this generation solar cells: monocrystalline silicon cell and polycrystalline silicon cell as shown in **Figure 3**. In terms of single-cell photovoltaic system, silicon solar cell is the most commonly used of all solar cells and it is the most effective. The highest efficiency of silicon solar cell was about 24% in large-area commercial [16] and about 25% in laboratory scale [17, 18]. However, silicon solar cells are costly to manufacture, thus research has pushed the next generation of solar cells away from silicon.

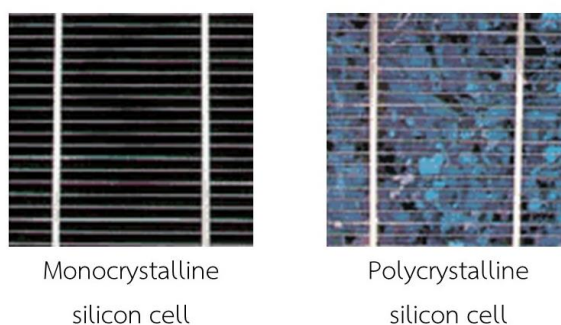


Figure 3: Silicon solar cells [19].

Second-generation solar cells are usually called thin-film solar cells. These solar cells are made from a few micrometers thick of semiconductor materials layers, so they are much cheaper than other solar cells. Its lower production costs and minimal material use of thin-film solar cells make them attractive to industry. Thin-film solar cells can be classified into 4 types depending on the type of absorber layer

used: a-Si, CdTe, CIGS, and CZTS solar cells. Although these thin-film solar cells have lower costs and good efficiencies, they have some drawbacks. a-Si solar cell has a significant degradation in the power output when they are exposed to the sun. CIGS solar cells are made of increasingly rare and expensive elements (indium and gallium) while CdTe solar cells are made of highly toxic element (cadmium). Due to these disadvantages, a new generation of solar cells has been inspired.

Third-generation solar cells are made from a variety of new materials, both organic and inorganic material. The goal of these solar cells is to achieve high efficiency and less expensive devices. These solar cells include dye-sensitized solar cells, perovskite solar cells, quantum dot solar cells, and organic solar cells. At present, the most challenging issue in these solar cell is the long-term stability [20].

2.2 Thin-Film Solar Cells



Thin-film solar cells were originally introduced in the 1970s. The advantage of these solar cells is composed of micro-thick absorbing material layers which lead to low production cost. The working of thin-film solar cells relies on substances known as semiconductors which are consisted of p-type (high concentration of hole or deficiency of electron) and n-type (high concentration of electron) semiconductors. A combination of p-type and n-type semiconductor together form the p-n junction which is fundamental to the function of a solar cell. The p-n junction act as an electric field. When sunlight reaches the absorber layer, photons with energy greater than band gap of the semiconductor are absorbed by the cell. The electron is then excited from the valence band to the conduction band, producing electron-hole pair. The electrons migrate to the n-type side of the junction while the holes migrate to the p-type side of the junction because of the electrostatic force of the field across the junction. Generally, a solar cell consists of negative front contact and positive back contact. A semiconductor p-n junction is between these two contacts. If the two contacts are connected by an external circuit, current will start flowing from positive to negative terminal of the solar cell as shown in **Figure 4**.

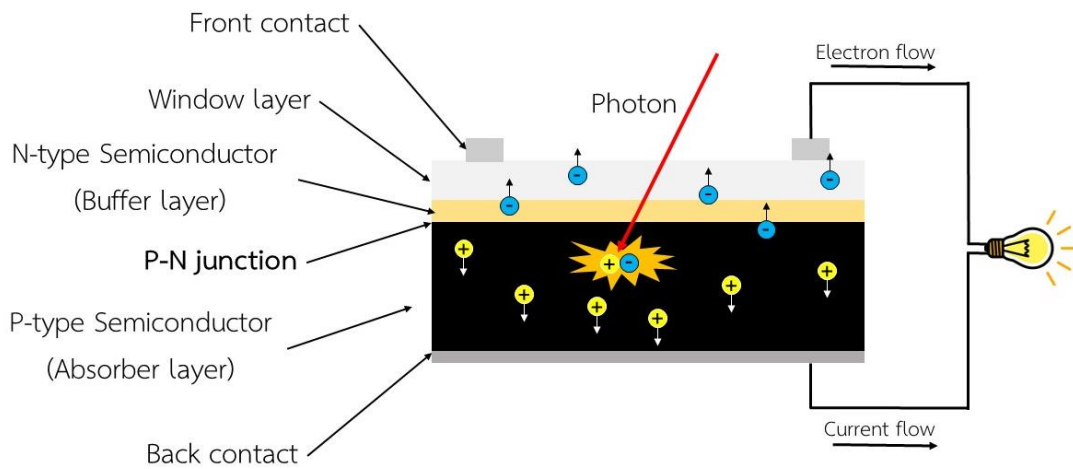


Figure 4: Working principle of a solar cell [21].

Nowadays, there are 3 types of thin-film solar cells in the market which are amorphous a-Si, CdTe, and CIGS. a-Si is the oldest thin-film technology. It consists of non-toxic element. In addition, it can absorb a wide range of the light spectrum and performs well in low light. However, a-Si has a significant degradation in the power output when they are exposed to the sun resulting in loses efficiency quickly. The highest efficiency on record for a-Si is only 10.3% [1]. CdTe is the most common thin-film solar technology, largely because of utility-scale applications. CdTe solar cell has the highest efficiency of 22.1% [1]. However, there are health concerns regarding the use of cadmium in thin-film solar cells because cadmium is a highly toxic element. CIGS solar cell has the highest efficiency of 22.6% [2]. However, a large-scale production of this thin-film is limited because of the less availability and cost of the material (indium and gallium). Currently, researchers are focusing on the development of the new quaternary material CZTS which is composed of earth-abundant and non-toxic element. CZTS has an optimal energy band gap of around 1.5 eV and high absorption coefficient ($>10^4 \text{ cm}^{-1}$) [3], making the CZTS suitable for the light absorption layer in thin-film solar cells.

2.3 Copper Zinc Tin Sulfide

CZTS is a p-type semiconductor which has received increasing interest since the late 2000s for thin-film solar cell application. CZTS offers optical and electrical properties similar to the CIGS, making it well suited for light absorption layer in thin-film solar cell. Moreover, CZTS is composed of only abundant and non-toxic elements which are copper (Cu), zinc (Zn), tin (Sn), and sulfur (S).

From the chalcopyrite CIGS structure, one can obtain CZTS by substituting the trivalent In/Ga with a bivalent Zn and IV-valent Sn which forms in the kesterite structure, the lowest energy of CZTS structure. Some literature reports have identified CZTS in the related stannite structure, but conditions under which a stannite structure may occur are not yet clear. The kesterite and stannite structure of CZTS are shown in **Figure 5**. The kesterite and stannite structure are differed the location of Cu and Zn [22]. In this work, the pure kesterite CZTS structure will be synthesized.

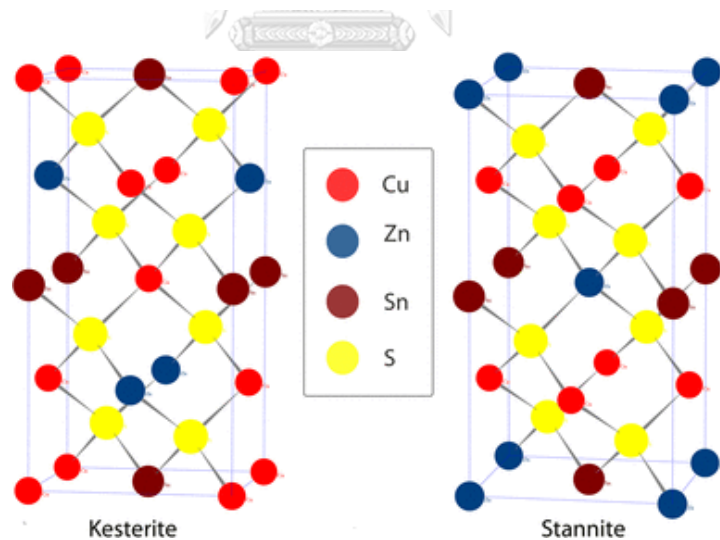


Figure 5: Crystal structures of CZTS [23].

2.3.1 Copper Zinc Tin Sulfide Synthesis

In general, CZTS thin-film can be synthesized by both physical processes and chemical processes as summarized in **Figure 6** [24, 25].

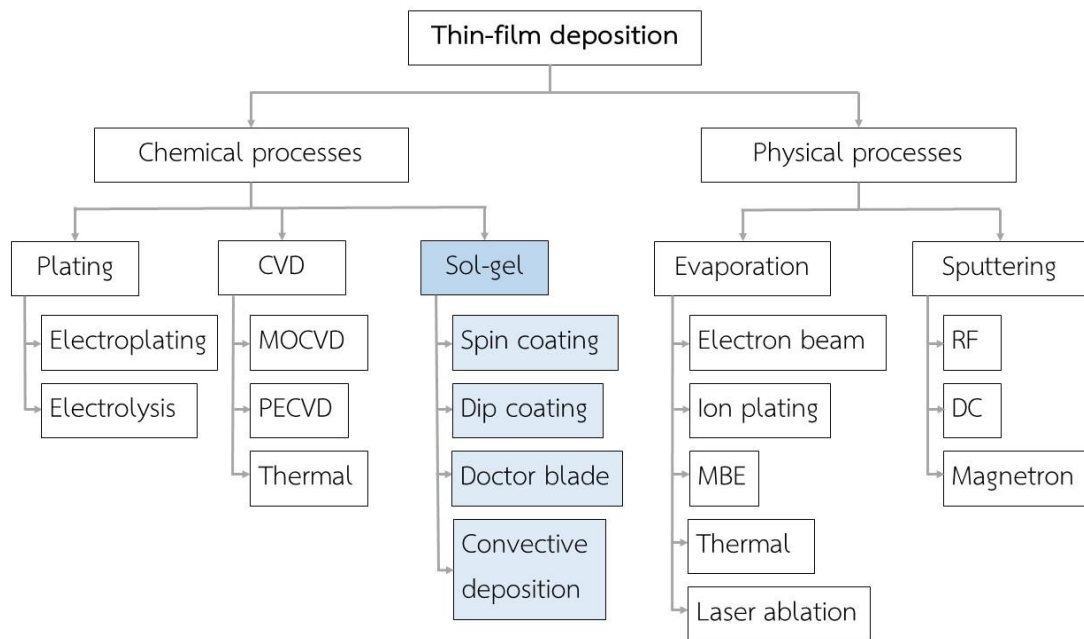


Figure 6: Thin-film deposition techniques.

The advantages of the film synthesized using the physical processes e.g. sputtering, and evaporation are smooth, dense, non-porous, and large grain size, which is highly efficient when used to fabricate the solar cell. Moreover, the physical processes don't require the use of specialized chemicals as used in chemical vapor deposition (CVD). However, these processes relatively expensive. In addition, some chemical processes such as CVD must be performed under a vacuum environment, resulting in high production costs. Nowadays, the researchers are interested in a low-cost and non-vacuum process, a solution-based process. The solution-based process is more suitable for industrial-scale mass production. The CZTS thin-film solar cell synthesized using the solution-based method has the highest efficiency of 12.6% by using hydrazine as a solvent [26] and 12.7% by applying $\text{In}_2\text{S}_3/\text{CdS}$ layer over the CZTSSe film and using hydrazine as a solvent [27]. Although the use of hydrazine as a solvent led to high efficiency CZTS thin-film solar cells, they have some problems. Hydrazine is a highly toxic substance and probably carcinogenic. Therefore, the CZTS synthesized using hydrazine as a solvent is not suitable for industrial production. Currently, the research has focused on a solution-based process using a less expensive and benign solvent.

In general, the synthesis of CZTS thin-film using a solution-based method has many defects in the film e.g. holes and crack. These defects could be caused during thin-film deposition, solvent evaporation process, and annealing process. Holes and crack formation in the film cause the electron-hole recombination resulting in decrease in the efficiency of solar cells. In addition, the synthesis of CZTS thin-film using a solution-based method yields less efficiency as result of smaller grain size and porous film. Therefore, the CZTS thin-film must be improved after the deposition process to obtain high thin-film quality (high crystallinity, dense, and large grain size). One of the most possible ways to improve the crystallinity is annealing in sulfur or selenium atmosphere which is called sulfurization or selenization process. Ziti et al. synthesized the CZTS thin-film using the sol-gel process and deposited on a substrate by spin coating technique. The study of the annealing temperature in a range of 300 to 350°C found that the crystallinity increases when the annealing temperature was increased [4]. In addition, the film quality is improved by synthesizing a film from a mixture of CZTS precursor solution and CZTS nanoparticles CZTS, a hybrid solution. The nanoparticles were exploited to promote grain growth while the precursor solution was exploited to homogenize the CZTS thin-film. Wang et al. found that the combining of CZTS nanoparticles and CZTS precursor solution results in higher crystallinity of the CZTS film and higher efficiency of the solar cell [6, 7]. They reported efficiency of 4.92% when deposited CZTS precursor solution on the nanoparticles film [6] and 6.39% when the film was fabricated using the CZTS hybrid solution [7]. However, the process of CZTS nanoparticles deposition is quite difficult.

In addition to this, doping by using alkali metals e.g. Li, Na, K, and Rb is one of the ways to enhance the film quality. Doping in CZTS thin-film has been proved to be positive effects such as promoting crystal growth, reducing point defects, reducing the secondary phase, increasing p-type carrier concentration, and passivating the grain boundaries [8-12] resulting in increasing solar cell efficiency [28]. In this thesis, Na-doped in CZTS thin-film was focused.

2.3.2 Na-Doping in CZTS Thin-Film

Na-doping in CZTS thin-film can be done both after thin-film deposition and during thin-film deposition. Moreover, it can be done by both physical processes such as sputtering method and chemical processes such as sol-gel method. Sun et al. fabricated CZTS thin-film using sputtering method and Na-doped post-treatment by deposited NaF layer with 0, 10, and 20 nm thickness on the CZTS film. The results showed that 10 nm of NaF layer was proved to be optimal thickness. As shown in **Figure 7**, the CZTS film without Na addition demonstrates the smallest grain size compare with other samples. While the CZTS film with 10 nm NaF layer demonstrates the larger grains and dense film. Moreover, there are no void or pinholes in this film. However, the CZTS film with 20 nm NaF layer demonstrates some pinholes and void on the film which may cause shunt resistance problems in the solar cell. The solar cell efficiency was 3.07%, 4.10%, and 2.78% by doping with 0, 10, and 20 nm NaF layer, respectively, which is consistent with the morphology of the films. It can be concluded that the pinholes and void in the CZTS film causes a decrease in solar cell efficiency [29]. The appropriate absorber layer for thin-film solar cell must be dense, smooth, no void or pinholes in order to achieve the highest efficiency.

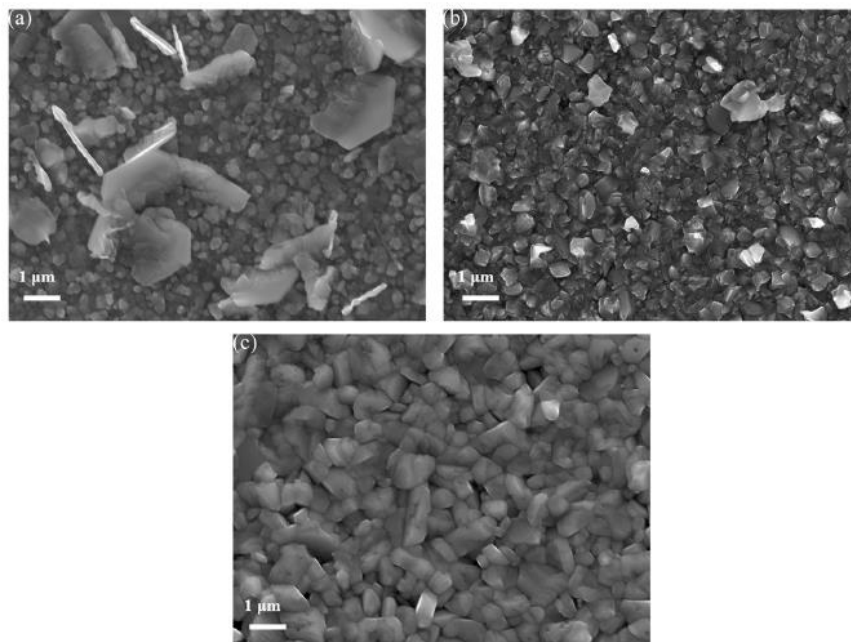


Figure 7: SEM images of CZTS thin-films with 0 nm (a), 10 nm (b), and 20 nm (c) of NaF.

In addition, there are some research have been conducted on the Na-doping in the CZTS thin-films using chemical process such as sol-gel method. Laghfour et al. have investigated the impact of Na incorporation in CZTS thin-film using sol-gel spin coating method. NaCl which was used as a Na source, was mixed in the CZTS sol-gel solution at 0%, 10%, 20%, and 30% NaCl to CZTS molar ratio and deposited on a substrate by spin coating method. The results found that 10% molar doping have the best structure quality because it has the highest intensity at (112) plane as shown in **Figure 8**. Moreover, it was found that the energy band gap of CZTS films was decreased from 1.45 to 1.34 eV with increasing the Na incorporation from 0% to 30% molar, respectively. The decrease of the energy band gap is attributed to Na induced defects located inside the energy band gap [9].

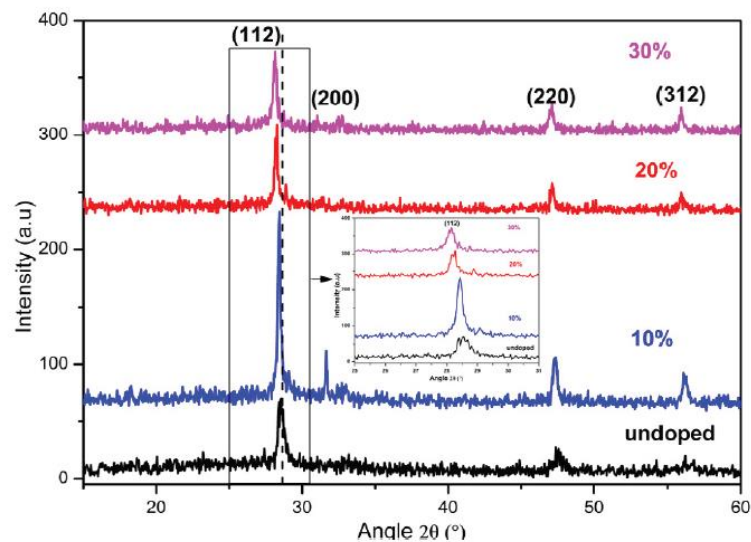


Figure 8: XRD patterns of CZTS thin-film doped with 0%, 10%, 20%, and 30% of Na.

Tong et al. synthesized the CZTS thin-film using sol-gel and spin coating method. They also improve the CZTS film quality by doping with Na. Na_2CO_3 was doped into the film by mixing in the CZTS sol-gel solution at the range from 3.9% to 5.4%. By observing the morphologies, average grain sized was enlarged apparently when Na-concentration increase. The best film quality was obtained by doping with 4.8% Na-doping. As shown in **Figure 9**, the grain size is increased while pinholes and grain boundaries are decreased compared to 3.9% and 4.3% Na-doping. However,

doping with 5.4% demonstrates the inhomogeneous growth which leads the appearance of pinholes. The CZTS solar cell with 4.8% Na-doping has the highest J_{SC} improvement with efficiency of 2.92% which is consistent with the film morphologies [30].

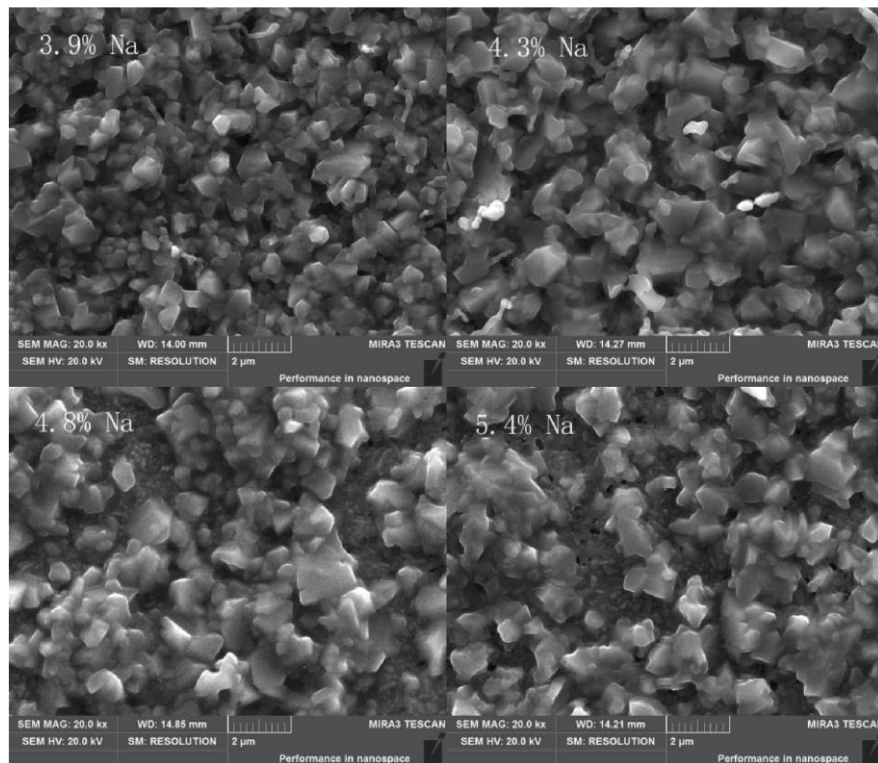


Figure 9: SEM images of CZTS thin-films with 3.9%, 4.3%, 4.8%, and 5.4% Na-doping.

In addition to the Na-doped during thin-film deposition, there are some research that dope the Na into the CZTS film after thin-film deposition. Duan et al. prepared the CZTSSe thin-film using sol-gel and spin coating method. The Na was doped into the CZTS thin-film by depositing the NaCl solution on a CZTS film. The Na incorporation in CZTS thin-film lead to dense and smooth films with large grains as shown in **Figure 10**. Moreover, it was found that the deposition of NaCl layer on the CZTS film beneficial for the formation of a p-n junction. This is because the copper vacancy (V_{Cu}) is generated from cation substitutions such as Na_{Cu} and Na_{Zn} which may occur during the Na-doping. V_{Cu} on the CZTSSe surface will be occupied by Cd^{2+} during the CdS deposition process, leading to the formation of a homogenous p-n junction. The Na-doped CZTSSe solar cell was achieved the highest efficiency of 11.18% by

doping with 5 mg/ml of NaCl solution, the average efficiency has increased by more than 13% from 9.45% (undoped) to 10.71% [8].

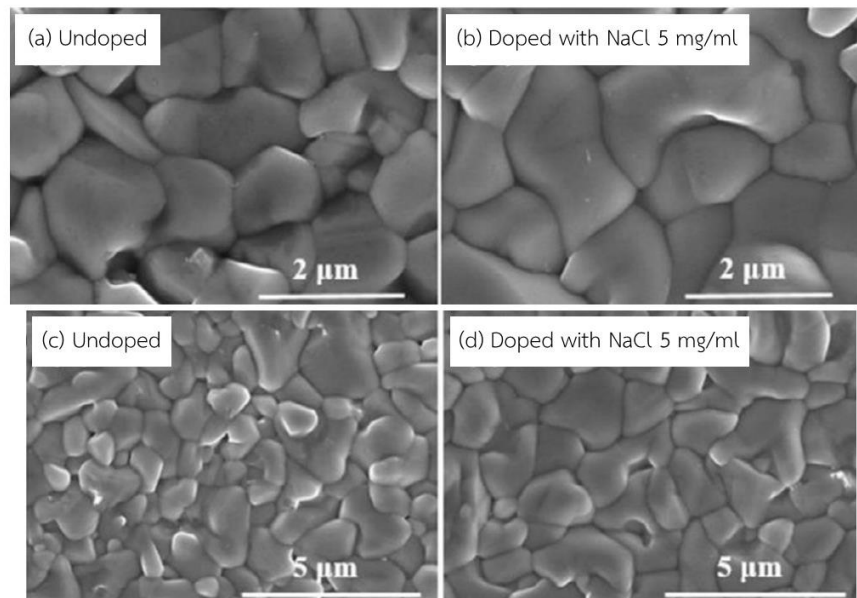


Figure 10: SEM images of the CZTSSe film (c, e) and 5 mg/ml Na-doped CZTSSe films (d, f).

From the previous research, it can conclude that the Na incorporation in the CZTS film affects the properties of the CZTS film which is beneficial to the CZTS solar cells. Na-doping in CZTS film enlarge the grain size, decrease the grain boundaries pinholes, and roughness surface. Moreover, Na-doping in CZTS thin-film increase the carrier concentration, leading to increase the current. These properties lead to higher solar cell efficiency.

In this thesis, the CZTS thin-films were synthesized using the sol-gel convective deposition technique and the properties of the film were improved by doping with Na. The effects of Na-doping concentration and doping methods were investigated in terms of structural properties (grain size, crystal size, and roughness surface), optical property (optical band gap), and solar cell characteristics (V_{OC} , J_{SC} , and FF).

2.3.3 CZTS synthesis using the Sol-gel Technique

The sol-gel process which is known as a chemical solution process is a method for the synthesis of solid materials from small molecules. It is one of the most popular

methods for CZTS synthesis because it is easy to control the chemical composition and microstructure of the film, simple equipment, and low-cost. The sol-gel process consists of the preparation of the sol, successive gelation, and solvent removal, which is based on the hydrolysis or alcoholysis and polycondensation reactions of the metal precursors. After polycondensation reactions, the sol which is a colloidal suspension of particles in the solution is observed. The sol is deposited on the substrate to form a thin-film by using a general deposition technique. During the solvent removal, the gelatinous network is formed on a substrate which is called gel or xerogel film. After the annealing process, a solid thin-film is obtained as shown in **Figure 11**.

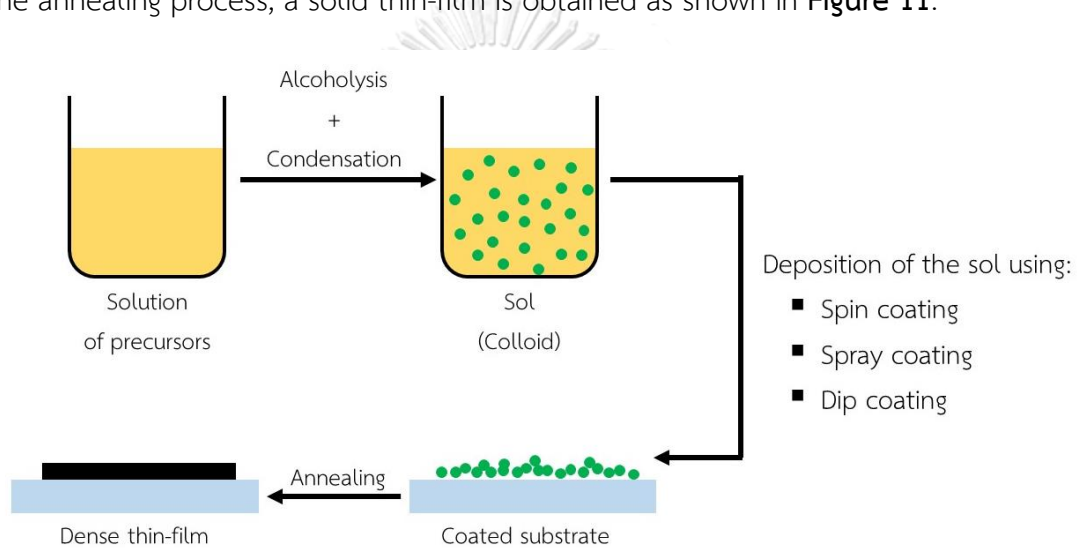


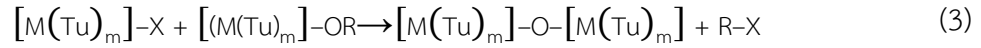
Figure 11: Thin-film deposition using the sol-gel method [31].

In this thesis, a CZTS sol-gel solution was synthesized by using 2-methoxyethanol as a solvent, which can be described as follows [32]:

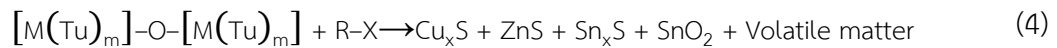
Firstly, metal salts react with thiourea to form metal-thiourea complex.



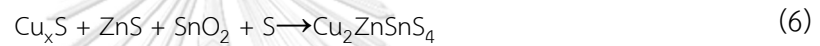
Then, the metal-thiourea complex is subjected to alcoholysis and polycondensation reactions with 2-methoxyethanol to form the sol as described in equation 2 and 3, respectively. The sol is deposited on a substrate to form a sol thin-film by using a general deposition technique such as spin coating, spray coating, and convective deposition.



The sol film is then converted into xerogel film during a gelation and solvent evaporation process. At the same time, the binary metal sulfides and oxides are formed because the thermal decomposition of thiourea-metal-oxygen complex.



The formation of CZTS are also involved in this process.



M represents metal ions which are Cu^{2+} , Zn^{2+} , and Sn^{2+} , X represents anion such as CH_3COO^- and Cl^- , Tu is thiourea, and R is organic molecular chains of 2-methoxyethanol. In the sol-gel process, there are many parameters that affect the film quality such as the concentration of precursor solution, heating temperature. Therefore, the process must be properly controlled to achieve the high film quality.

2.3.4 Deposition Method for CZTS Solution

The CZTS sol-gel solution can be deposited to form a thin layer solution on a substrate by general coating methods such as spin coating, dip coating, spray coating, doctor blade coating, and convective deposition technique. Each technique has different strong point and weak point as follow:

2.3.4.1 Spin Coating

Spin coating is the simplest method for fabricating a thin-film on a substrate. The coating process is started by drop the solution on a substrate. The substrate is then spun using centrifugal force at high speed to spread the solution, forming a thin-film solution on a substrate. The thickness of the film depends on the spinning speed,

spinning time, viscosity, concentration and volume of the solution. Spin coating process consists of 4 steps which are (1) deposition, (2) spin-up, (3) spin-off, and (4) evaporation, as shown in **Figure 12**. An interesting feature of the spin coating technique is easy to control the film thickness by adjusting the spinning speed and time. Moreover, the deposited film is quite uniform and smooth. However, it requires a large amount of solution and produces a lot of solution wastage. Most importantly, this technique is not suitable for large-scale mass production.

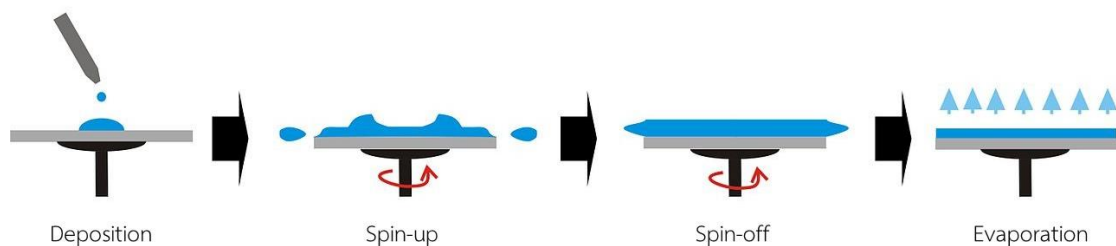


Figure 12: Graphical representation of spin coating technique [33].

2.3.4.2 Dip Coating

Dip coating is a thin-film deposition technique, which is suitable for complex shapes and curved parts. The deposition process is started by immersing a substrate into the precursor solution. Then, the substrate is lifted vertically from a solution, forming a thin-film solution layer on the substrate. After that, the solvent is evaporated, resulting in a thin-film on the substrate as shown in **Figure 13**. Despite its simple and low cost, but it is slow and required a lot of precursor solution. Moreover, the precursor solution may be easily contaminated.

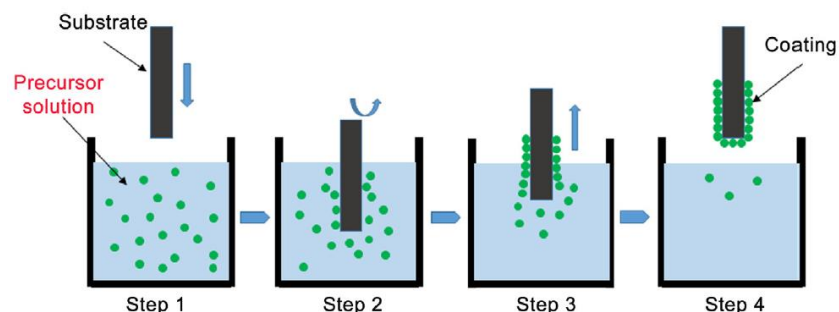


Figure 13: Graphical representation of dip-coating technique [31].

2.3.4.3 Spray Coating

Spray coating is a thin-film deposition process by spraying the solution onto a substrate as shown in **Figure 14**. Spray coating is a quick, effective, and economical method. However, it is difficult to control the thickness and requires a very expensive apparatus, which can result in a high cost.

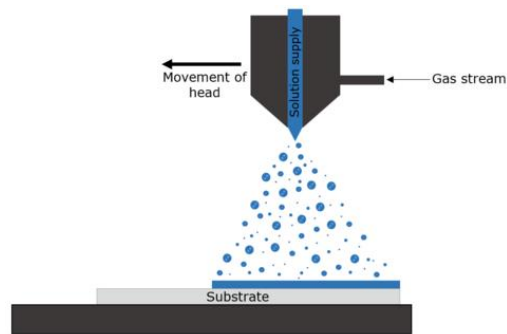


Figure 14: Graphical representation of spray coating techniques [34].

2.3.4.4 Doctor Blade Coating

Doctor blade coating is one of the widely used methods for thin-film deposition on a large area production. In this process, the solution is plated on a substrate beyond the blade. When the blade is moved with constant speed, the solution is spread on the substrate forming a thin-film layer as shown in **Figure 15**. The advantage of this method is easy to control the thickness by adjusting the gap between the blade and the substrate. However, it requires a high viscous solution to form a film.

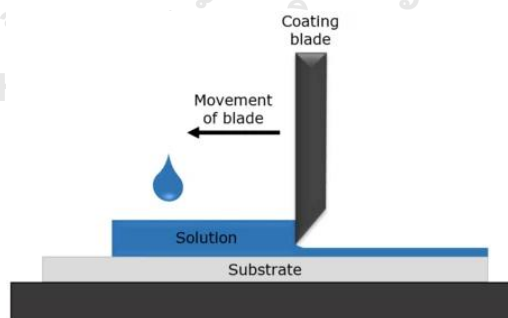


Figure 15: Graphical representation of doctor blade coating techniques [34].

2.3.4.5 Convective Deposition

The convective deposition is an alternative method to fabricate a thin-film. It uses the capillary force to pull the solution on a moving substrate resulting in a thin-film layer. The advantage of this method is easy to control the thickness by adjusting

the deposition speed. The convective deposition requires just a few micrometers of precursor solution to produce a uniform film and produces very low material wastage. In addition, it has high-throughput production which is suitable for coating on large areas.

2.4 Convective Deposition Technique

The convective deposition is an alternative method that is suitable for a thin-film fabricating on a nanometer scale. In this process, the precursor solution is injected between the deposition blade and the substrate. Then the solution is spread out and held between the deposition blade and the substrate by the capillary force. The deposition blade is stationary while the glass substrate moves with constant speed to the right. During the substrate is pulled horizontally, the solution is held by the capillary interaction resulting in a uniform thin layer of solution on the substrate. After solvent evaporation, a thin solid film is obtained as shown in **Figure 16**. In general, this method is used to fabricate a monolayer film colloidal by using convective assembly. In the convective deposition technique, the film thickness is controlled by adjusting the deposition speed and the concentration of the precursor solution. As the concentration of precursor solution increases, the film thickness will increase. On the other hand, the deposition speed increases, the film thickness will decrease [35].

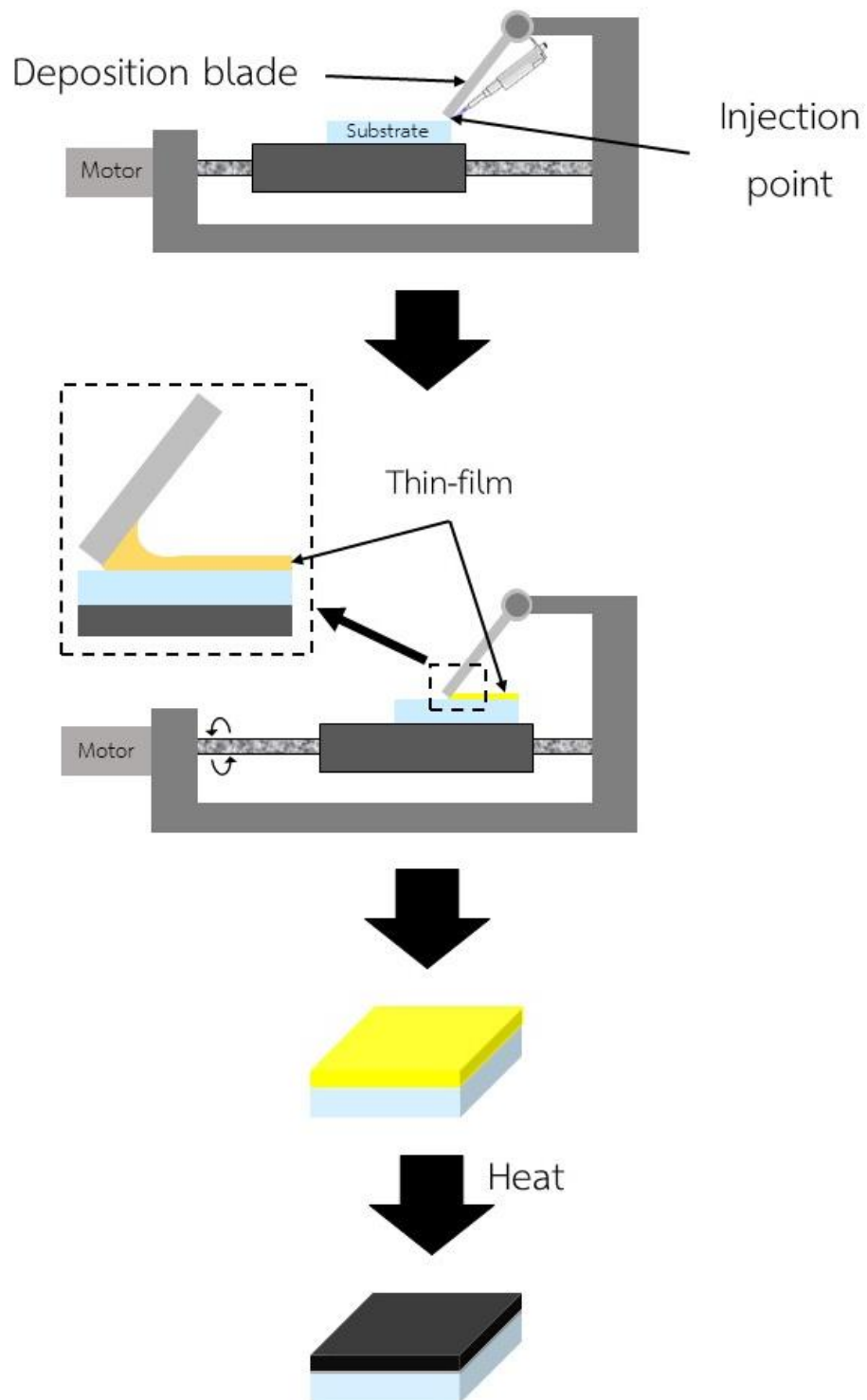


Figure 16: Convective deposition technique.

There are several parameters in the convective deposition process that affect the properties of the film such as the deposition speed, deposition temperature, pre-

heating temperature, annealing temperature, and the precursor concentration. These parameters must be properly controlled to achieve a high film quality. Chonsut et al. compared the film quality in terms of thickness, crystallinity, surface morphology, and absorption behavior. The study was found that the convective deposition technique provides comparable properties to that fabricated by the spin coating method. Moreover, they found that a film was prepared by using the convective deposition technique requires a significantly smaller amount of the precursor solution compares to the spin coating method [36]. Therefore, the convective deposition is a good candidate method to be applied for thin-film fabrication in both laboratory and industrial scale.

2.5 CZTS Thin-Film Solar Cell Structure

In general, the CZTS thin-film solar cells consist of 6 components as shown in **Figure 17**, from bottom to top;

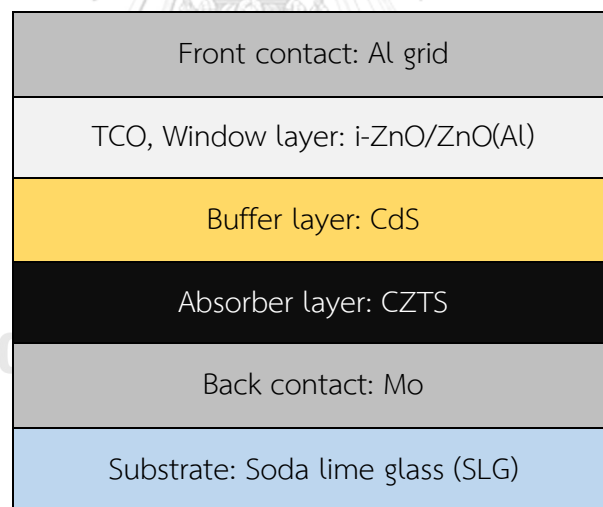


Figure 17: Schematic of CZTS thin-film solar cell structure.

2.5.1 Substrate

The substrate is used to support the other layers of CZTS thin-film solar cells. Soda-lime glass (SLG) is generally used for a substrate in CZTS thin-film solar cell due to it has well-matched thermal expansion coefficient as CZTS. Moreover, SLG has high thermal stability which allows process temperature up to 600°C.

2.5.2 Back contact

The function of the back contact layer is charge carrier collection and conduction during solar cell operation. In addition, it acts as an optical reflector to reflect the light to the absorber layer in the CZTS thin-film solar cell. In general, Molybdenum (Mo) is widely used as a back contact because it does not react strongly with CZTS and it is chemically stable during CZTS synthesis [37].

2.5.3 Absorber layer

The main purpose of the absorber layer is to absorb photons. In this work, CZTS which is a new film absorber was used as an absorber layer in CZTS thin-film solar cell. The reason CZTS has been one of the promising absorber layers for thin-film solar cells because it is a low-cost, earth-abundant, and non-toxic element. Moreover, CZTS has optimal band gap energy around 1.5 eV and has a large absorption coefficient over 10^4 cm^{-1} . The absorber layer must have a large grain and dense film in order to achieve high efficiency of solar cell.

2.5.4 Buffer layer

The purpose of the buffer layer is to provide an intermediary between the absorber layer and the window layers. The CIGS and CZTS thin-film solar cells are generally used cadmium sulfide (CdS) as a buffer layer because it is the most reliable and gives the best performance solar cell.

2.5.5 Window layers

The window layer should have wide band gap energy to minimize optical losses and maximize photon transmission and have high conductivity in order to maximize conduction and minimize the series resistance. The window layers normally consist of the high resistance intrinsic zinc oxide (i-ZnO) and the low resistance aluminum doped zinc oxide (ZnO(Al)).

2.5.6 Front contact

The benefit of front contact is increasing the collection of electrical current. In general, Al is used as a front contact due to its high electrical conductivity, low-cost, high abundance, and low density. High electrical conductivity to mass ratio could be highly beneficial especially thin film solar cells, where grid metals make a larger part of the device mass.

2.6 Characteristics of Solar Cell

The solar cells are generally measured in terms of a current-voltage (I-V) curve as shown in **Figure 18**. The basic characteristics of a solar cell are the short-circuit current, the open-circuit voltage, the fill factor, and the solar energy conversion efficiency. Each parameter is described as follows:

2.6.1 Short-circuit current (I_{sc})

Short circuit current is the maximum current which may be drawn from the solar cell. Short circuit current occurs when the voltage across the solar cell is zero.

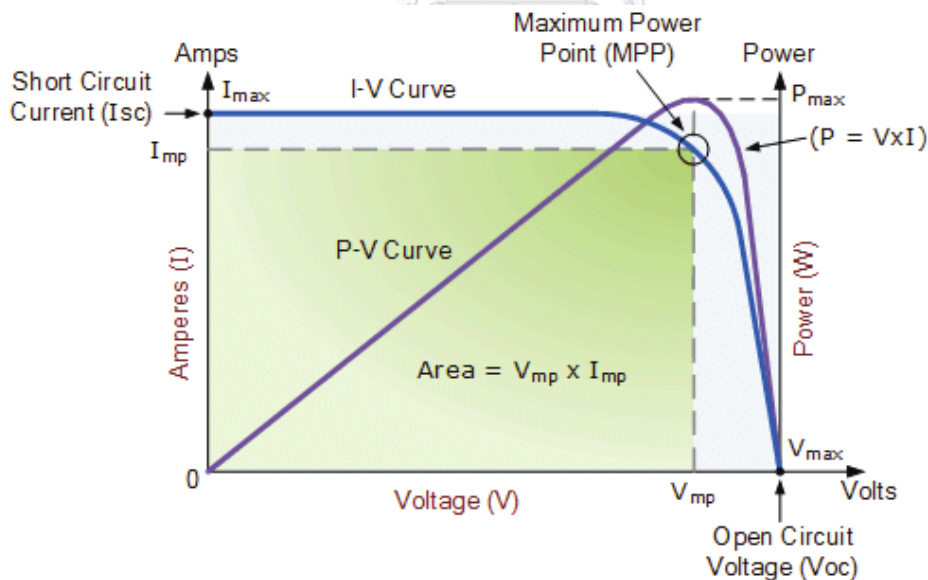


Figure 18: I-V and P-V characteristics of a typical solar cell [38].

2.6.2 Open-circuit voltage (V_{oc})

Open-circuit voltage is the maximum voltage from a solar cell which occurs when the net current through the solar cell is zero.

2.6.3 Fill factor (FF)

Fill factor is the ratio of maximum power from the solar cell to the actually produces. The maximum power is obtained from the maximum current (I_{max}) multiplied by the maximum voltage (V_{max}), while the actual power is obtained from the short-circuit current and the open-circuit voltage. Hence:

$$FF = \frac{I_{max} \times V_{max}}{I_{sc} \times V_{oc}} \quad (7)$$

2.6.4 Solar cell efficiency (η)

The solar cell efficiency is defined as the ratio of energy output from the solar cell to input energy from the sun. The solar cell efficiency depends on the solar cell temperature and the incident sunlight intensity. Therefore, conditions under which efficiency is measured must be carefully controlled in order to compare the performance of one device to another. In general, solar cells are measured under AM 1.5 conditions and at a temperature of 25°C. The efficiency of a solar cell is defined as:

$$\eta = \frac{I_{max} \times V_{max}}{P_{light}} = \frac{I_{sc} \times V_{oc} \times FF}{P_{light}} \quad (8)$$

CHAPTER 3

EXPERIMENTAL

In this chapter, the steps for preparation the CZTS thin-films and fabricating the CZTS thin-film solar cells are present. First, the details of CZTS thin-films synthesis are explained. Then, the steps for preparation the CZTS solar cell are described. Finally, the analyzed instrument for the CZTS thin-film and the CZTS thin-film solar cells are briefly described.

3.1 Synthesis of CZTS Thin-Films

The steps for synthesis of CZTS thin-films consisted of preparation of CZTS precursor solution, preparation of Na-doped CZTS precursor solution, and preparation of NaCl solution. These solutions were used to fabricated 3 types of CZTS thin-films which are 1) CZTS thin-film, 2) CZTS/NaCl (CZTS thin-film doped by deposited NaCl solution on CZTS thin-film), and 3) CZTS+NaCl (CZTS thin-film doped by mixing NaCl in CZTS precursor solution), as summarized in **Figure 19**.

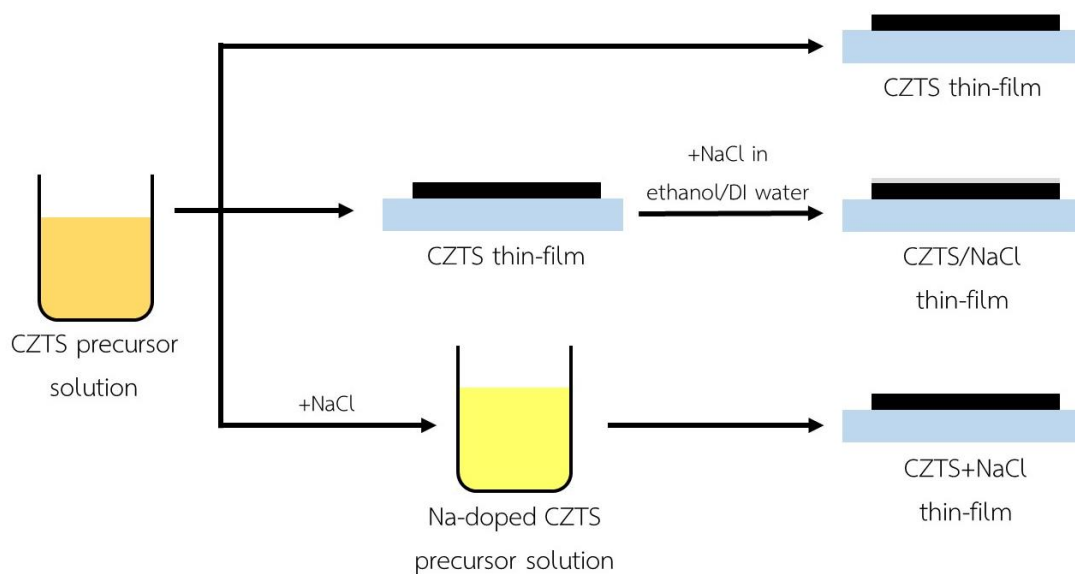


Figure 19: Preparation of undoped and Na-doped CZTS thin-films.

3.1.1 Chemicals

1. Copper (II) chloride ($\text{CuCl}_2 \cdot 2\text{H}_2\text{O}$) from CARLO ERBA Reagents
2. Zinc (II) chloride (ZnCl_2) from Himedia Laboratories
3. Tin (II) chloride ($\text{SnCl}_2 \cdot 2\text{H}_2\text{O}$) from CARLO ERBA Reagents
4. Thiourea ($\text{SC}(\text{NH}_2)_2$) from Himedia Laboratories
5. 2-methoxyethanol ($\text{C}_3\text{H}_8\text{O}_2$), 99.5% from CARLO ERBA Reagents
6. Monoethanolamine (MEA; $\text{C}_2\text{H}_7\text{NO}$), 99.0% from LOBA Chemie
7. Sodium Chloride (NaCl), 99.9% from Ajax Finechem
8. Ethanol ($\text{C}_2\text{H}_5\text{OH}$), 99.9% from Quality Reagent Chemical

3.1.2 Preparation of CZTS Precursor Solution

First, ZnCl_2 (0.31 M) was dissolved into 20 ml of 2-methoxyethanol. Then, $\text{CuCl}_2 \cdot 2\text{H}_2\text{O}$ (0.48 M) and $\text{SnCl}_2 \cdot 2\text{H}_2\text{O}$ (0.25 M) were dissolved into the previous solution. The solution was stirred and heated at 50°C . After that, 0.5 ml of MEA and 2 M of thiourea were added into the previous solution. A clear yellow solution was obtained after an hour stirring at 50°C .

3.1.3 Preparation of Na-Doped CZTS Precursor Solution

NaCl was used as a Na source and it was dissolved to the CZTS precursor solution with 5%, 10% and 15% molar ratios of NaCl to CZTS to form Na-doped CZTS precursor solutions. In this thesis, CZTS+5, CZTS+10 and CZTS+15 are referred to Na-doped CZTS thin-film by mixing 5%, 10% and 15% molar ratios of NaCl to CZTS in CZTS precursor solution, respectively.

3.1.4 Preparation of NaCl Solution

5, 10 and 15 mg of NaCl were dissolved in 10 ml of deionized water and ethanol mixed solvent (volume ratio 1:1). These solutions were used to deposit on CZTS thin-films by convective deposition to form Na-doped CZTS thin-film. Similarly, CZTS/5, CZTS/10 and CZTS/15 are referred to Na-doped CZTS thin-film by deposited 5, 10 and 15 mg/ml NaCl solution on CZTS thin-film, respectively.

3.1.5 Deposition of CZTS Thin-Film

CZTS precursor solution was deposited on a substrate using convective deposition technique. The schematic illustration of equipment set-up is shown in **Figure 20**. First, 30 μl of CZTS precursor solution was injected to the injection point (between the substrate and the deposition blade). Then the substrate was pulled horizontally at 500 $\mu\text{m/s}$ to form a thin layer of the solution on the substrate. After that, the CZTS thin-film solution was pre-heated on a hot plate to remove the solvent at 200°C for 10 minutes. The deposition and pre-heating processes were repeated 15 times to obtain desired thickness about 1 μm . For Na-doped thin-film by deposited NaCl solution on CZTS thin-film, 30 μl of NaCl solution was deposited on the CZTS thin-film by convective deposition and pre-heated on a hot plate at 200°C for 10 minutes. Finally, CZTS thin-films with and without Na-doping were annealed under nitrogen atmosphere at 550°C for 30 minutes.

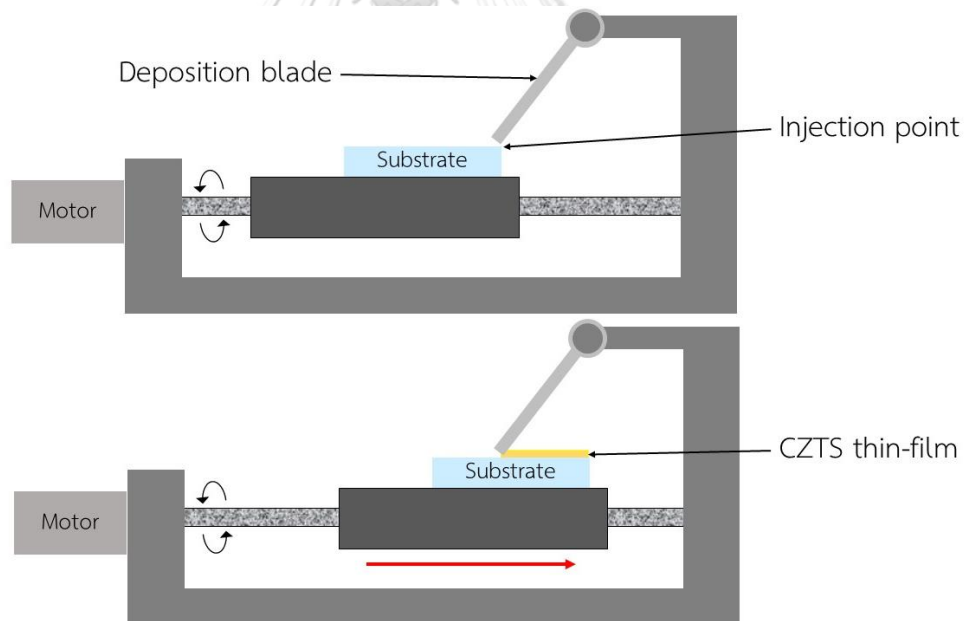


Figure 20: Thin-film deposition using convective deposition technique.

3.2 Fabrication of CZTS Thin-Film Solar Cell

The steps for fabricating CZTS thin-film solar cell are summarized in **Figure 21**. The details of each step are explained as follow:

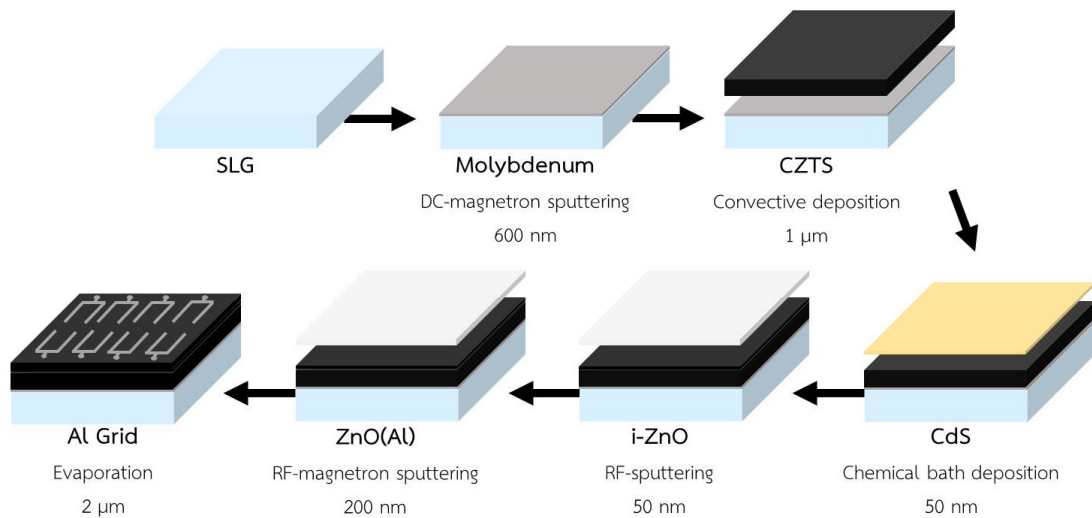


Figure 21: Schematic of CZTS thin-film solar cell fabrication.

3.2.1 SLG Substrate Preparation

3x3 cm² SLG was used as a substrate. The SLG preparation step is started by soaking the SLG in dishwashing detergent with deionized (DI) water for 24 hours in order to remove dust and grease from the glass surface. Then, rub the SLG with a sponge and clean it with DI water. After that, soak the SLG in a mixture of Decon-90 and DI water for an hour at 60°C in an ultrasonic bath. The next step is cleaning with DI water and soaking the SLG in chromic acid for an hour in order to create the sough surface before depositing the film. Finally, the SLG is sonicated in DI water and dried with nitrogen gas.

3.2.2 Mo Deposition

Mo was used as a back contact material for CZTS thin-film solar cell. The thickness of Mo back contact layer is about 600 nm. The Mo back contact layer was deposited on SLG by DC magnetron sputtering using 4-inch in diameter 99.95% Mo target under 6×10^{-3} mbar of argon atmosphere with a sputtering power of 550 W for 11 minutes with sample rotation speed at 3 rpm.

3.2.3 CZTS Thin-Film Deposition

CZTS was used as an absorber layer with a thickness around of 1 μm. CZTS was deposited on Mo coated SLG using sol-gel convective deposition with a deposition

speed of 500 $\mu\text{m/s}$. Then, the film was dried on a hotplate in air at 200°C for 10 minutes. These steps were repeated for 15 times. Finally, the film was annealed in nitrogen atmosphere at 550°C for 30 minutes.

3.2.4 CdS Deposition

CdS is a buffer layer which is deposited on CZTS film using chemical bath deposition (CBD) technique. The CdS solution was prepared by using cadmium sulfate (CdSO_4), thiourea ($\text{SC}(\text{NH}_2)_2$), and ammonia solution (NH_4OH). The amount of each solution is summarized in **Table 1**. The CdS deposition is started by soaking CZTS thin-film in CdS solution at 65°C for 15 minutes with 150 rpm stirring. Finally, the films were rinsed with DI water and dried with nitrogen gas. The thickness of CdS layer is about 50 nm.

Table 1: The amount of chemicals used in chemical bath deposition.

Chemicals	Quantity
CdSO_4	0.3456 g + 50 ml DI water
$\text{SC}(\text{NH}_2)_2$	2.85 g + 100 ml DI water
NH_4OH	80 ml
DI water	270 ml

3.2.5 i-ZnO Deposition

i-ZnO is a window layer. The thickness of this layer is about 50 nm. i-ZnO layer was deposited on the CdS layer by RF sputtering using a i-ZnO target in 6×10^{-3} mbar of argon atmosphere with a sputtering power of 40 W for 20 minutes.

3.2.6 ZnO(Al) Deposition

ZnO(Al) is a window layer. The thickness of this layer is about 200 nm. ZnO(Al) layer was deposited on the i-ZnO layer by RF magnetron sputtering using a 2wt.% Al_2O_3 doped ZnO target in 3×10^{-3} mbar of argon atmosphere with a sputtering power of 220 W for 16 minutes with sample rotation speed at 3 rpm.

3.2.7 Al Grid

Al grid is used as a front contact. The metal Al grid was evaporated through a shadow mask which covers all area except the area to be deposited using the thermal evaporation technique at vacuum pressure. The thickness of Al grid is about 2 μm .

3.3 Analytical Instruments

The CZTS thin-films and CZTS solar cells were characterized to determine the chemicals composition, crystal structure, grain size, morphology, roughness surface, and efficiency using instruments as follows:

3.3.1 X-ray Diffraction (XRD)

XRD was used to investigate the crystal structures and phase formation of CZTS thin-films. Bruker AXS Model D8 Discover was operated at 5°/minutes of scan speed with 40 kV of operating voltage and 40 mA of current by using $\text{CuK}\alpha$ radiation source. The XRD patterns were collected by 2θ scan mode from 20° to 80°.

3.3.2 Scanning Electron Microscope (SEM)

SEM was used to investigate the grain size and morphology of CZTS thin-films. The JEOL JSM-7001F SEM with a wide range of magnification of 100x to 40,000x was used in this study.

3.3.3 Energy Dispersive X-ray Spectroscopy (EDS)

The JEOL JSM-7001F SEM with EDS was used to measure the chemical composition of CZTS thin-films in this study.

3.3.4 Atomic Force Microscopy (AFM)

AFM was used to measure the surface morphology and roughness surface of CZTS thin-films. The Veeco model Dimension 3100 was used in this study.

3.3.5 UV-Visible Spectrophotometer

A UV-Vis spectrophotometer (Shimadzu UV-2600) was used to determine the optical property of CZTS thin-films in terms of optical band gap. The wavelength range used in this study was from 300 to 1100 nm.

3.3.6 Current-Voltage Characteristics

Open-circuit voltage (V_{oc}), short-circuit current density (J_{sc}), fill factor (FF) and solar cell efficiency were measured under the light radiation of AM 1.5 at 25°C. Xenon arc lamp was used as a light source with the power density of 100 mW/cm². The area of solar cell was about 0.515 cm².



CHAPTER 4

RESULTS AND DISCUSSION

In this thesis, the CZTS thin-films were synthesized using sol-gel convective deposition method for use as an absorber layer in CZTS thin-film solar cell. The CZTS thin-films were doped with Na to improve the absorber layer properties in order to make it more suitable for the CZTS solar cell. The aim of the study is to investigate the effects of Na-doping on properties of the CZTS thin-films and CZTS thin-film solar cells. The studies were divided into 3 parts which are (1) effects of Na-doping on structural properties, (2) effects of Na-doping on optical property, and (3) effects of Na-doping on the solar cell performance. In this work, Na was doped into a CZTS thin-film by 2 methods: (1) deposited a NaCl solution on a CZTS thin-film by convective deposition, (2) mixed a NaCl in CZTS solution and deposited on a substrate by convective deposition. Each doping method use different Na concentrations as summarized in **Table 2**.

Table 2: Na concentration on the CZTS thin-films.

Samples	Doping method	mol Na
		(Cu+Zn+Sn)
CZTS/5	Deposited 5 mg/ml of NaCl solution on CZTS film	0.55%
CZTS/10	Deposited 10 mg/ml of NaCl solution on CZTS film	1.07%
CZTS/15	Deposited 15 mg/ml of NaCl solution on CZTS film	1.62%
CZTS+5	Mixed 5 %mol NaCl/CZTS in CZTS solution	0.30%
CZTS+10	Mixed 10 %mol NaCl/CZTS in CZTS solution	0.60%
CZTS+15	Mixed 15 %mol NaCl/CZTS in CZTS solution	0.90%

In general, the CZTS thin-film synthesis using solution-based process must be followed by high temperature annealing process in nitrogen atmosphere for better crystallization. **Figure 22** presented the XRD patterns of as-CZTS and annealed CZTS thin-films. The results shown that the (112) peak intensity become sharp and stronger

after annealing process. The sharp and stronger peak indicated the crystallinity and crystallite size of the annealed film was better compared to the as-CZTS thin-film. The crystallite sizes were estimated from XRD peak using Debye-Scherrer's equation as follow:

$$D = \frac{0.9\lambda}{\beta \cos\theta} \quad (9)$$

Where D is the crystallite size, λ is the wavelength of X-ray radiation used (1.5406 \AA), β is full width half maximum (FWHM), and θ is the Bragg angle. Moreover, the (112) peak intensity become stronger when increase the annealing temperature from 440°C to 550°C . Therefore, annealing process with 550°C was performed after thin-film deposition in order to achieve the best crystallinity.

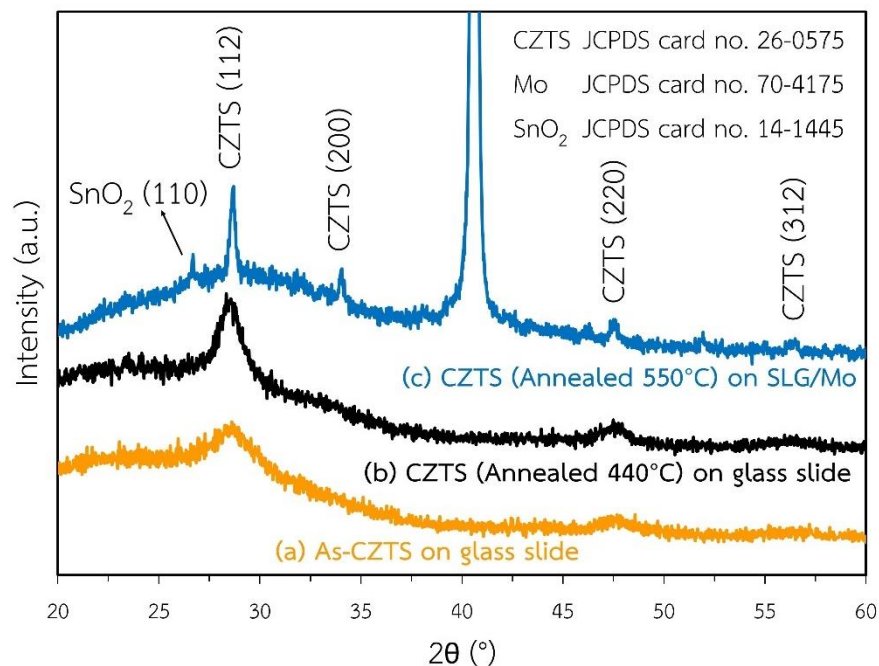


Figure 22: The XRD patterns of as-CZTS and annealed CZTS thin-films. The annealed films were performed in N_2 atmosphere for 30 minutes. The film thickness is about 300 nm.

In addition to high temperature annealing process, alkali doping in CZTS thin-film is one of the most possible ways to enhance grain size and solar cell performance.

In this work, the effects of Na-doping in CZTS thin-film fabricated by sol-gel convective deposition were investigated.

4.1 Na-doping Effects on Structural Properties of CZTS Thin-Film

In CIGS thin-film solar cells, an important factor which leads to high efficiency CIGS solar cells is copper vacancy (V_{Cu}) intrinsic defect. The V_{Cu} defect act as shallow acceptor producing less perturbation [9]. However, the dominant defect in CZTS is Cu_{Zn} defect due to similar atomic sizes of Cu and Zn lead to substitution of Cu atom instead Zn atom in the lattice [39]. Cu_{Zn} antisite defect is the deep surface or bulk defects, which limited the V_{OC} and the solar cell performance [22, 40]. To favor V_{Cu} formation over Cu_{Zn} defect, a Cu-poor Zn-rich condition was employed for the CZTS synthesis. In general, theoretical expected stoichiometric composition of $Cu_2Zn_5Sn_4$ or CZTS is Cu:Zn:Sn:S equal to 25.0:12.5:12.5:50.0 (in terms of at%) or 2:1:1:4. But in this work, the stoichiometric composition ratio of Cu/(Zn+Sn) and Zn/Sn were adjusted to 0.85 and 1.25, respectively in order to favor the V_{Cu} defect and to reduce the Cu_{Zn} defect.

First of all, the chemical composition of CZTS thin-films, which were synthesized using sol-gel convective deposition method and were annealed in N_2 atmosphere at $550^\circ C$ for 30 minutes was investigated to confirm the formation of CZTS at stoichiometric composition near 2:1:1:4 and to confirm the CZTS growth in Cu-poor Zn-rich condition. The chemical composition and composition ratios were present in **Table 3** and **Table 4**, respectively. The results clearly revealed that all samples were grown in Cu-poor Zn-rich condition ($Cu/(Zn+Sn) < 1$ and $Zn/Sn > 1$) with stoichiometric composition close to 2:1:1:4. Moreover, the presence of Na indicates the successful doping in the CZTS thin-films. The 3.58 at% of Na in the undoped CZTS thin-film was detected because of the diffusion of Na from SLG substrate into the film. However, there are some loss of sulfur which may occur during high temperature annealing process.

Table 3: Chemical composition of undoped and Na-doped CZTS thin-films.

Samples	Composition (At%)				
	Cu	Zn	Sn	S	Na
CZTS	21.18	16.51	11.82	46.91	3.58
CZTS/5	18.95	15.91	13.60	44.98	6.56
CZTS/10	20.24	14.31	14.73	45.92	4.80
CZTS/15	24.94	15.41	11.67	42.29	5.69
CZTS+5	25.79	16.89	12.31	41.11	3.89
CZTS+10	18.27	17.08	9.57	43.94	11.14
CZTS+15	22.23	15.01	10.97	46.35	5.45

Table 4: Element ratios of undoped and Na-doped CZTS thin-films.

Samples	Cu:Zn:Sn:S				Ratio		
	Cu	Zn	Sn	S	Cu/(Zn+Sn)	Zn/Sn	S/(Cu+Zn+Sn)
Defined					0.85	1.25	1.00
CZTS	1.79	1.40	1.00	3.97	0.75	1.40	0.95
CZTS/5	1.39	1.17	1.00	3.31	0.64	1.17	0.93
CZTS/10	1.37	0.97	1.00	3.12	0.70	0.97	0.93
CZTS/15	2.14	1.32	1.00	3.62	0.92	1.32	0.81
CZTS+5	2.09	1.37	1.00	3.34	0.88	1.37	0.75
CZTS+10	1.91	1.78	1.00	4.59	0.69	1.78	0.98
CZTS+15	2.03	1.37	1.00	4.23	0.86	1.37	0.96

In order to confirm the formation of the CZTS in kesterite phase and to explore the influence of Na incorporation on the kesterite phase, the CZTS thin-films were analyzed by XRD. The XRD patterns of undoped CZTS and Na-doped CZTS thin-films which were annealed at 550°C in N₂ atmosphere for 30 minutes were shown in **Figure 23**.

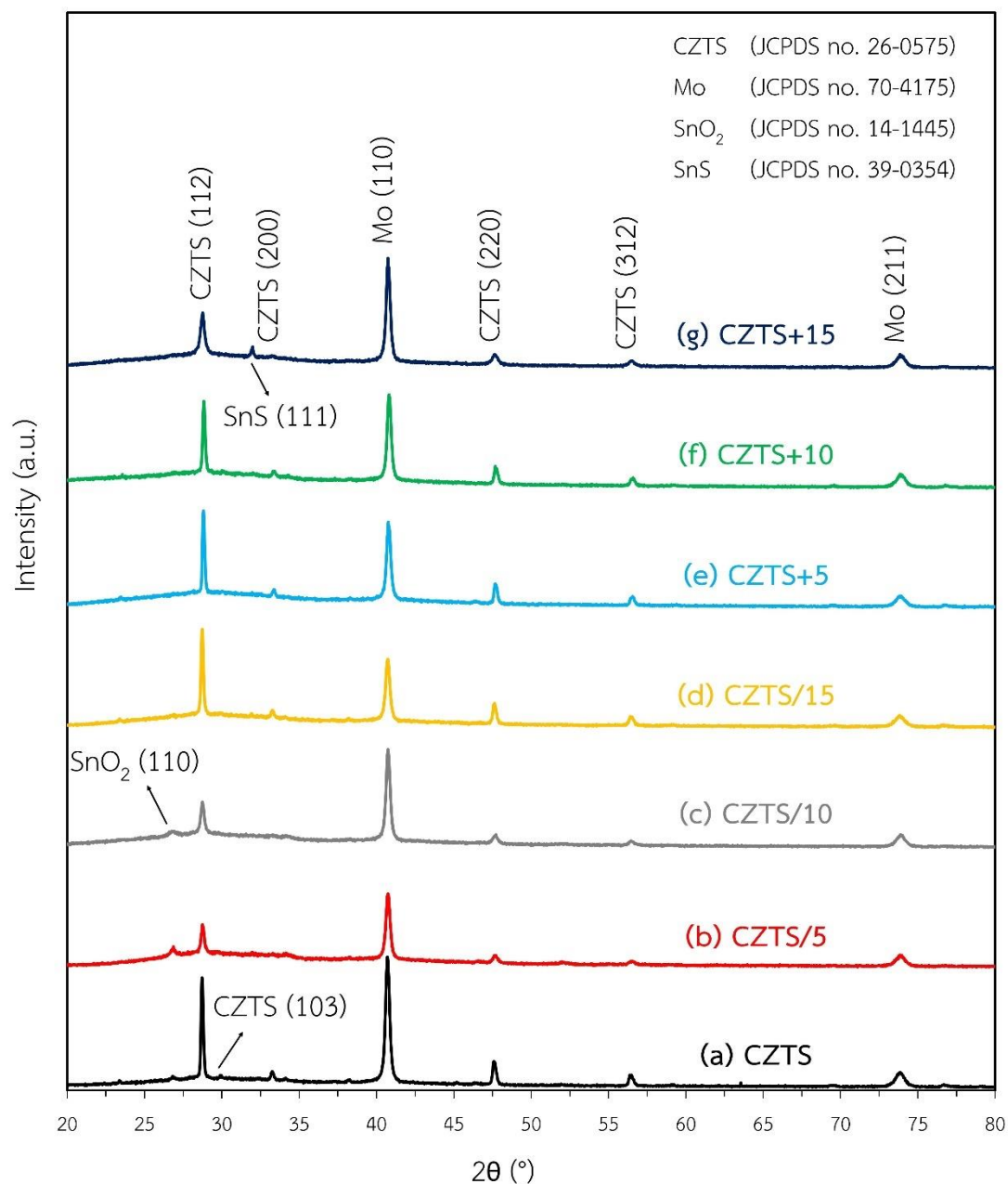


Figure 23: The XRD patterns of undoped and Na-doped CZTS thin-films. The films were annealed at 550°C in N₂ atmosphere for 30 minutes. The film thickness is about 1.2 μm.

The undoped CZTS film (**Figure 23 (a)**) is exhibiting the diffraction peaks located at 28.72°, 29.94°, 33.26°, 47.60°, and 56.49°, which are assigned respectively to the (112), (103), (200), (220), and (312) crystal planes of kesterite CZTS structure. These XRD patterns are in good agreement with the Joint Committee on Powder Diffraction Standard (JCPDS) card number 26-0575. From this result, it can be concluded that the

CZTS in kesterite phase was successfully synthesized by using sol-gel convective deposition method with annealing process at 550°C for 30 minutes. In addition, other peaks of the undoped CZTS film located at 40.71° and 73.83° are attributed to (110) and (211) planes of molybdenum (JCPDS card no. 70-4175), respectively. However, CZTS is a quaternary compound, thus numerous secondary phases can be found in the film. There is the peak located at 26.81° which is assigned to (110) plane of tin oxide (SnO₂) (JCPDS card no. 14-1445). SnO₂ secondary phase may occur during preheating and annealing process as described in equation (1) to (6). The SnO₂ has an energy band gap around 3.6 eV which is relatively large compared with the visible light. Thus, SnO₂ causes a reduced solar cell active area and decreases solar cell efficiency. The SnO₂ secondary phase was also observed in the CZTS/5 and CZTS/10, but not observed in CZTS/15 and the samples that doped by mixing NaCl in CZTS solution. This result is consistent with Zeng et al. report [41]. As Na-doping increase, the SnO₂ phase is decreased. Therefore, it can be concluded that the Na incorporation in CZTS thin-film could restrain the formation of SnO₂ secondary phase. Moreover, there is the peak located at 31.97° which is attributed to (111) planes of tin sulfide (SnS) according to JCPDS card no. 39-0354 in CZTS+15. SnS secondary phase has a low energy band gap around 1.1-1.3 eV. The lower energy band gap than CZTS risks to lower V_{OC}, thus it is detrimental for the solar cell performance. The concentration of Na in CZTS+15 may be too high leads to the substitution of Na atom instead of Sn atom. Thus, Sn²⁺ may be occupied by the excess S²⁻ leads to SnS formation [42]. Therefore, the doping with an appropriate amount of Na could restrain the formation secondary phase in CZTS thin-films.

By considering the Na-doped samples, there are the diffraction peaks located at 28.77°, 33.30°, 47.67°, and 56.53° for CZTS/5, the diffraction peaks located at 28.75°, 33.23°, 47.70°, and 56.45° for CZTS/10, the diffraction peaks located at 28.72°, 33.30°, 47.61°, and 56.43° for CZTS/15, the diffraction peaks located at 28.81°, 33.37°, 47.70°, and 56.56° for CZTS+5, the diffraction peaks located at 28.84°, 33.40°, 47.70°, and 56.61°, for CZTS+10, and the diffraction peaks located at 28.75°, 33.26°, 47.65°, and 56.50° for CZTS+15, which are assigned to the (112), (200), (220), and (312) planes of

kesterite CZTS structure, respectively. From this XRD results, there is no significant difference in XRD peak positions for all CZTS films, indicating that the sodium incorporation by both methods does not change the kesterite phase of CZTS absorbers. Moreover, the lattice parameters which were estimated based on tetragonal symmetry are also good agreement with the standard data of the kesterite structure. The lattice parameters and volume of unit cell of undoped and Na-doped CZTS film were summarized in **Table 5**. The results found that Na incorporation in the CZTS thin-film by both method does not significantly enlarge the lattice parameter and volume of unit cell of the CZTS.

Table 5: Lattice parameters and volume of unit cell estimated for the undoped and Na-doped CZTS film.

Sample	Lattice parameter (nm)		Volume of unit cell (Å ³)
	a=b	c	
JCPDS card no. 26-0575	0.548	1.085	319.5
CZTS	0.538	1.074	311.2
CZTS/5	0.538	1.072	309.8
CZTS/10	0.539	1.070	310.5
CZTS/15	0.538	1.077	311.2
CZTS+5	0.537	1.071	308.4
CZTS+10	0.536	1.070	307.7
CZTS+15	0.538	1.071	310.4

Although, there are no difference in peak positions for all samples, sodium incorporation in CZTS thin-films affect the peak intensity. By considering at the (112) plane of CZTS kesterite, it is clearly revealed that the peak intensity and peak width are different which indicate that the crystallinity of each samples are different. The crystallite sizes of were estimated from (112) plane of the XRD using equation (9). The corresponding XRD characteristics of (112) plane and the crystallite sizes are presented in **Table 6**.

Table 6: The corresponding XRD characteristics of (112) plane.

Samples	$2\theta_{(112)}$ (°)	$FWHM_{(112)}$ (°)	D (nm)
CZTS	28.72	0.16	50
CZTS/5	28.77	0.31	26
CZTS/10	28.75	0.31	26
CZTS/15	28.72	0.17	49
CZTS+5	28.81	0.16	53
CZTS+10	28.84	0.17	47
CZTS+15	28.75	0.37	22

The crystallite sizes obtained from Debye-Scherrer's equation are in the range of 22 to 53 nm. The highest crystallite size of 53 nm was obtained by doping with mixing 5% mol NaCl in the CZTS solution. On the other hand, the highest crystallite size of the sample which was doped by depositing NaCl solution on the CZTS thin-film was obtained by CZTS/15 with the crystallite size of 49 nm. While the crystallite size of undoped CZTS was 50 nm. As the XRD results, it was found that Na incorporation in the CZTS thin-film does not significantly enlarge the crystallite size. However, Na incorporation in the CZTS thin-film can affect the morphologies of the CZTS thin-film e.g. grain size, grain boundaries, and film roughness. These factors are a part to achieve high solar cell performance. The effects of Na incorporation on the thin-film morphologies will be discussed in the next topic.

The CZTS thin-film for use as an absorber layer in the CZTS thin-film solar cell must be dense, smooth, large grain size, without pinholes, without crack, and without secondary phase in order to achieve the highest solar cell efficiency. Therefore, the SEM and AFM images of CZTS thin-films were analyzed to investigate the film morphologies. The SEM images were used to compare the surface morphologies, grains size, pinholes, and crack of the undoped and Na-doped CZTS thin-films. **Figure 24** shows the surface SEM images of Mo coated on SLG and CZTS thin-films on the Mo-coated on SLG substrate. From the SEM images, it was found that all CZTS thin-films

were completely covered over the Mo layer. It can be concluded that the sol-gel convective deposition method is one of the efficient method to fabricate a thin-film. In addition. The results found that the Na incorporation in CZTS thin-films supports the growth of grains while the undoped CZTS thin-film has smaller grains size and nonuniform film compare to the Na-doped CZTS thin-film. For the undoped CZTS film (**Figure 24 (b)**), it demonstrates the inhomogeneous growth and agglomeration of the grains which leads the appearance of the pinholes and rough surface. In addition, there are some pinholes and grain boundaries in the film. The grains size of the undoped CZTS thin-film which was measured by the ImageJ program for 100 grains from 3 pictures was about 263 nm. As can be seen in **Figure 25 (a)**, grains size distribution of the undoped CZTS thin-film was broad and skewed to the right which means the inhomogeneous growth and most grains are small sizes.

For Na-doping in CZTS thin-film by depositing the NaCl solution on a CZTS thin-film, CZTS/5 and CZTS/10 (**Figure 24 (c) and (e)**) becomes more uniform compared to the undoped CZTS film, but still has small grain size. The grains size distribution of the CZTS/5 and CZTS/10 (**Figure 25 (b) and (d)**) were narrow and symmetry which means the uniform growth with average grain sizes of about 223 and 257 nm, respectively. These films still small grain size may be due to a small amount of Na could not enlarge the grains of CZTS film. When the Na concentration was increased to 15 mg/ml, the grain size and crystallinity were significantly improved. Moreover, the film is more continuous and more compact with a large average grain size of about 475 nm. The grains size distribution of the CZTS/15 (**Figure 25 (f)**) was a normal distribution which indicates that the growth of the grains is uniformity. In addition, the grain boundaries seem homogeneous because of Na diffuses to the grain boundaries by attaching with sulfur, resulting in the dense connection of the grains (**Figure 24 (g)**). CZTS/15 is the best film morphology in the case of Na-doping by depositing the NaCl solution on a CZTS thin-film, which is consistent with the XRD result.

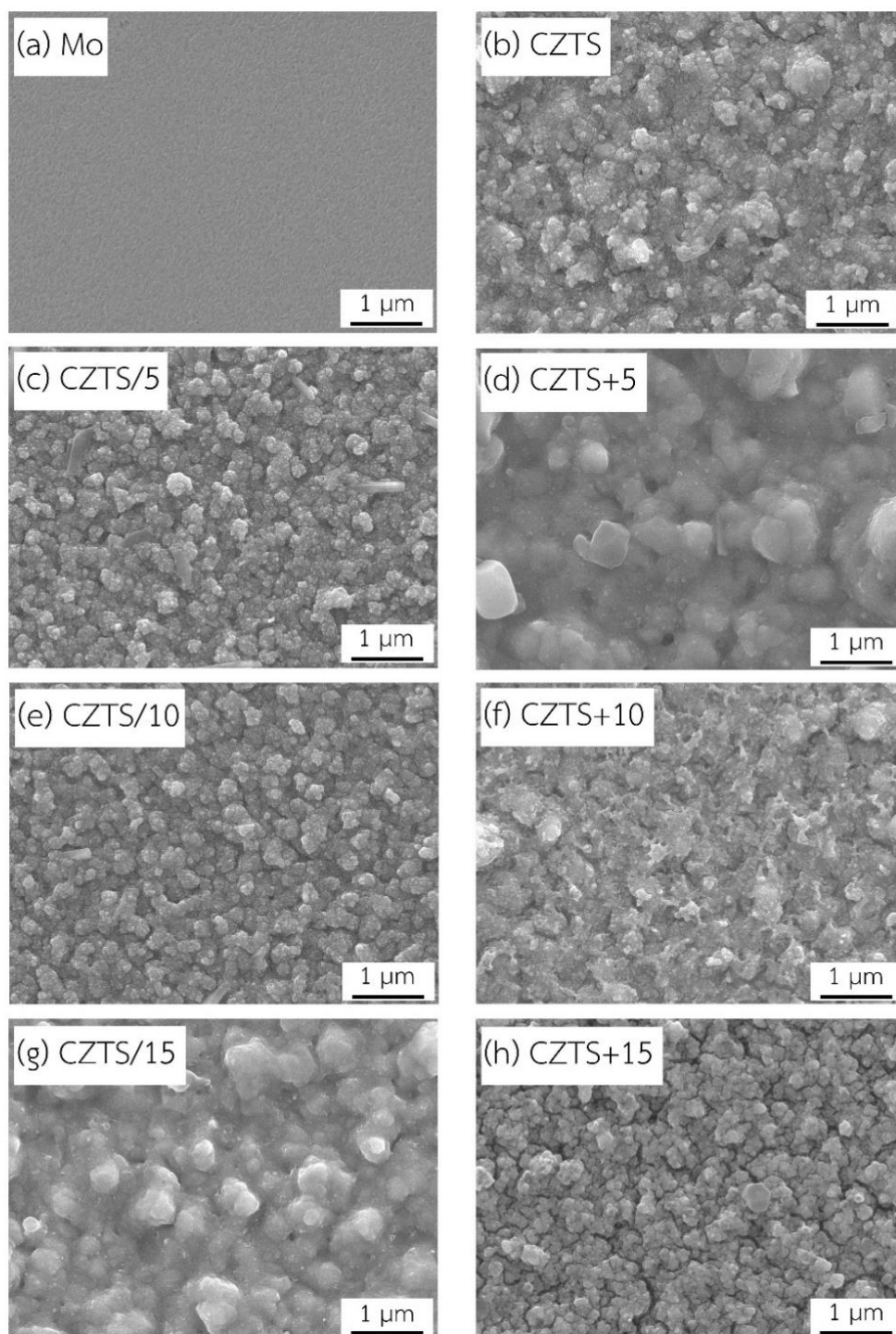


Figure 24: Top-view SEM images of undoped and Na-doped CZTS thin-films. The films were annealed at 550°C in N_2 atmosphere for 30 minutes. The film thickness is about 1.2 μm .

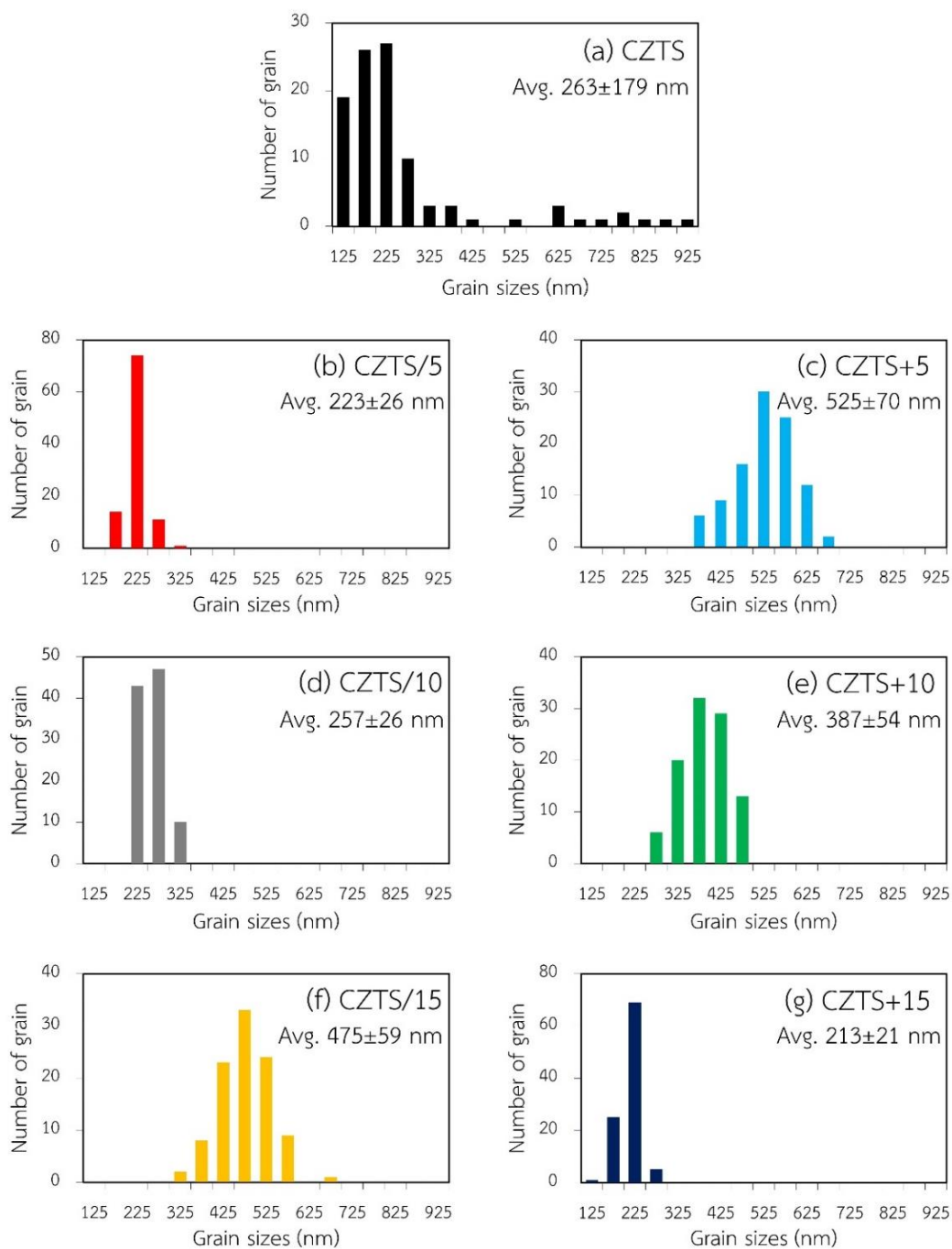


Figure 25: Grains size distribution of undoped and Na-doped CZTS thin-films. The grains size was measured by the ImageJ program for 100 grains from 3 pictures.

For Na-doping in CZTS thin-film by mixing NaCl in the CZTS solution, CZTS+5 demonstrates the larger grains without crack (**Figure 24 (d)**). In addition, the grain boundaries seem homogeneous because Na diffuse in between grain boundaries

surface lead to smoother and large grains [43]. The average grain size of CZTS+5 was about 525 nm with the normal distribution (**Figure 25 (c)**). However, when the Na-doping concentration is increased more than 10%, the grain size in the films become smaller (**Figure 24 (f) and (h)**). Moreover, some holes and crack were observed on the surface of CZTS+15. This may be because more sodium incorporation hampers the growth of CZTS. The grains size distribution of the CZTS+10 and CZTS+15 (**Figure 25 (e) and (g)**) were narrow which indicates that the growth of the grains is uniformity with average grain size of about 387 and 213 nm, respectively.

As mention above, the thickness of CZTS film must have enough volume to absorb the solar spectrum and generate electron-hole pairs. Therefore, the thickness about 1.2 μm was defined in this work. The CZTS film was deposited on a substrate layer by layer to measure the film thickness using SEM cross-sectional image. A layer of CZTS film is about 80 nm. Thus, 1.2 μm thickness needs to repeat the deposition process 15 times. The cross-sectional SEM images of undoped CZTS, CZTS/15, and CZTS+5 which was deposited 15 times by convective deposition technique were presented in **Figure 26**. The film thickness of the undoped CZTS was about 1248 nm with a standard deviation of 36 nm. The undoped CZTS film contains small grain, voids, and nonuniform growth. Moreover, it appears some crack and holes on the film surface. These defects in the film could lead to carrier recombination in the solar cell. By doping with Na, the films were densely packed and more uniform with a thickness of 1172 and 1198 nm with a standard deviation of 36 and 34 nm for CZTS/15 and CZTS+5, respectively. Na incorporation in CZTS thin-films may reduce the formation of agglomerates, resulting in uniformity and dense films. The dense and uniform film is beneficial for carrier transport leading to higher solar cell performance. Therefore, it can be concluded that the morphologies of Na-doped CZTS thin-film is better than the undoped film.

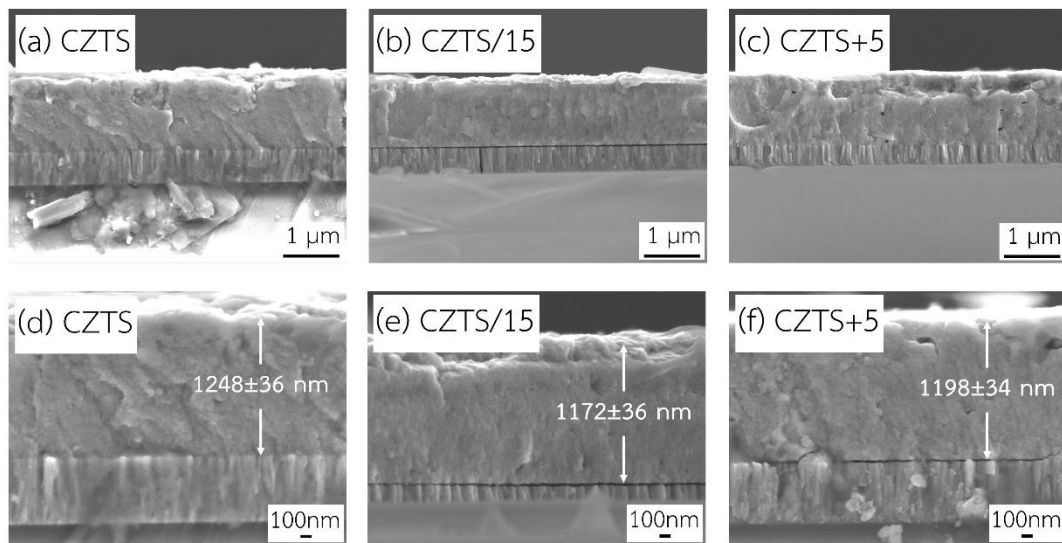


Figure 26: Cross-sectional SEM images of CZTS (a, d), CZTS/15 (b, e), and CZTS+5 (c, f) films.

The surface morphology and surface roughness of undoped and Na-doped CZTS films were further analyzed using AFM as shown in **Figure 27**. It was found that Na-doping in CZTS thin-films by both methods can reduce the surface roughness. The root means square (rms) roughness of undoped CZTS thin-film from AFM result was 68 nm while rms roughness of CZTS/15 and CZTS+5 was significantly decreased to 51 and 60 nm, respectively. The height profiles of 3 typical positions were shown in **Figure 27 (d-f)**. It was shown that the surface height of undoped CZTS was in the range of 250 to 300 nm while the surface height of CZTS/15 and CZTS+5 was reduced to 100 to 200 nm. From SEM and AFM analysis, it can be concluded that the Na-doping in CZTS thin-films could decrease the surface roughness and produce much smoother film compare to the undoped one. This smooth surface and is beneficial for p-n junction between the CZTS and CdS layers because it can reduce both the dark current and interfacial states in the solar cell [8].

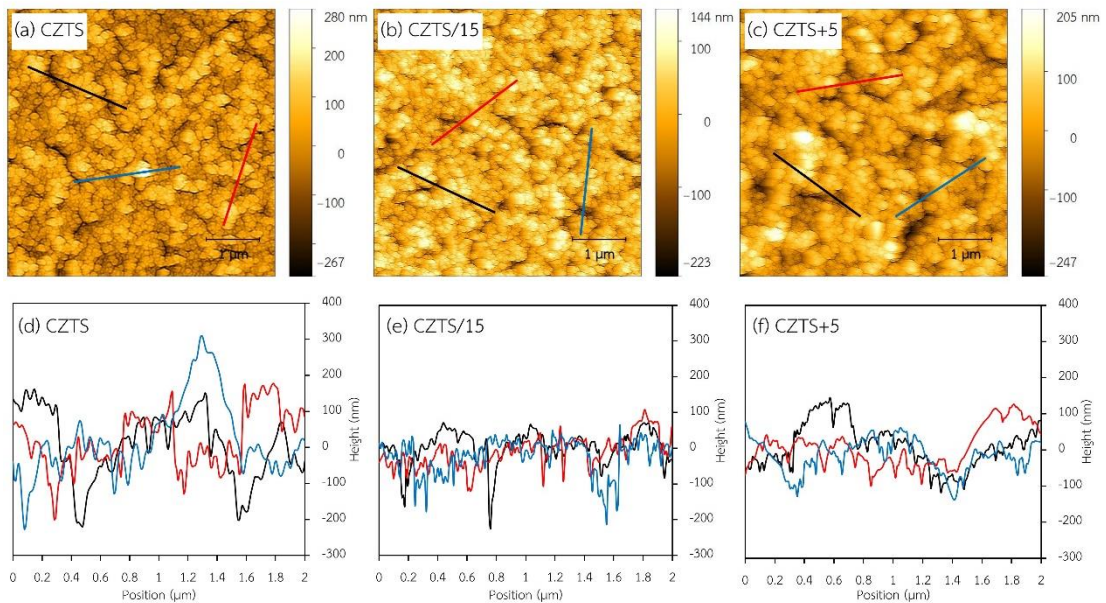


Figure 27: AFM images and height profiles of CZTS (a, d), CZTS/15 (b, e), and CZTS+5 (c, f) films.

4.2 Na-doping Effects on Optical Properties of CZTS Thin-Film

To investigate the optical properties of undoped and Na-doped CZTS thin-films fabricated by sol-gel convective deposition, UV-Vis spectrophotometer was done with the wavelength range of 300 to 1100 nm. The optical properties of the films were determined in terms of absorption coefficient and band gap. As shown in **Figure 28**, the absorption coefficients of the undoped and Na-doped CZTS thin-films have higher than 10^5 in the visible wavelength region which is good for the absorber layer in the solar cell.

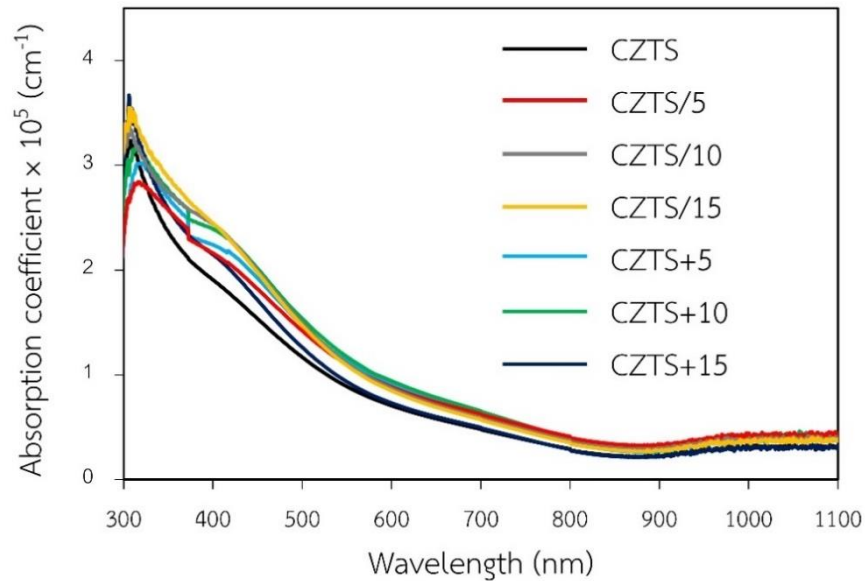


Figure 28: Plot of absorption coefficient of undoped and Na-doped CZTS thin-films.

The direct transition energy band gaps of undoped and Na-doped CZTS thin-films were estimated from the Tauc plot as following equation: $(\alpha h\nu) = A(E_g - h\nu)^n$, where α is absorption coefficient, h is Planck's constant, ν is frequency, A is constant, E_g is energy band gap, and n is equal to $1/2$ for direct transition. The Tauc plot and energy band gaps of CZTS thin-films are presented in **Figure 29**. The band gap of undoped CZTS thin-film was 1.60 eV. For Na-doped thin-films, the energy band gap reduces to range of 1.51-1.57 eV. The incorporation of sodium into CZTS film results in a lowering band gap because Na-induced defects located inside the band gap which agrees well with others' reports [9, 41]. In addition, energy band gap of a thin-film depends on the grain size, band gap is decreased with larger grain sizes. The energy band gap of the CZTS films in the range of 1.5 to 1.6 eV is consistent with the other reports and suitable for solar cell application.

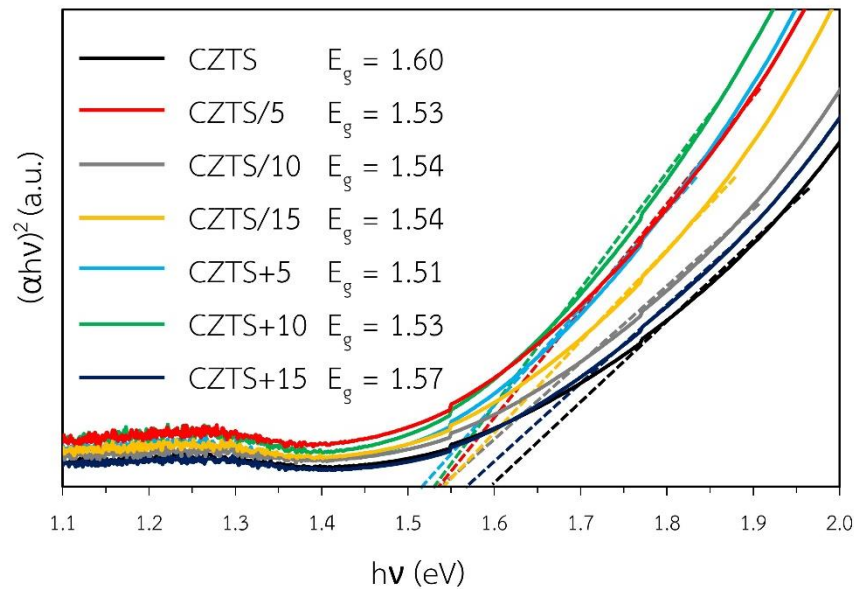


Figure 29: Tauc plot of $(\alpha h\nu)^2$ vs. photon energy ($h\nu$) of undoped and Na-doped CZTS thin-films. The dash line is extrapolated to determine energy band gap (E_g).

4.3 Na-doping Effects on the Solar Cell Performance

For solar cell fabrication, the 3 samples which are undoped CZTS, CZTS/15, and CZTS+5 were selected to use as an absorber layer in the CZTS thin-film solar cells with the structure of SLG/Mo/CZTS/CdS/i-ZnO/ZnO(Al)/Al. Photograph of each layers coated and final CZTS solar cell were presented in **Figure 30**. The CZTS solar cells were tested under the light radiation of AM 1.5 at 25°C with the power density of 100 mW/cm² in order to investigate the effects of Na incorporation on the solar cell performance.

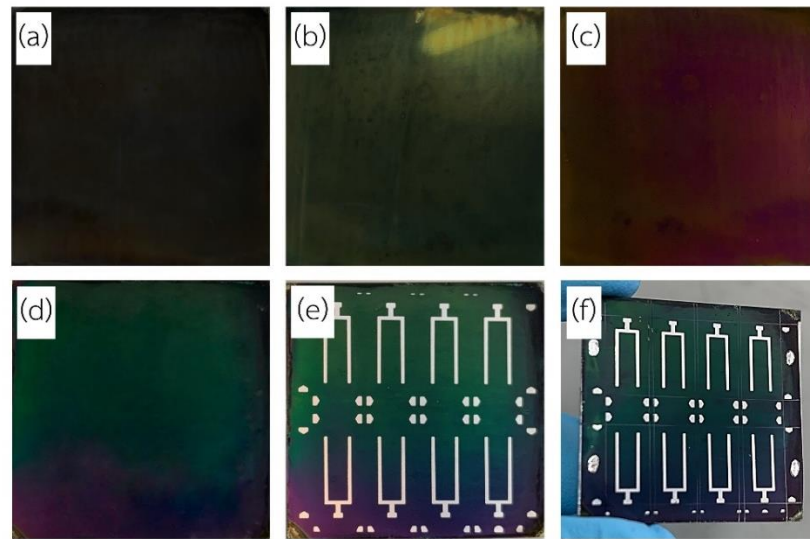


Figure 30: Photographs of CZTS thin-film on Mo coated SLG (a), SLG/Mo/CZTS/CdS (b), SLG/Mo/CZTS/CdS/i-ZnO (c), SLG/Mo/CZTS/CdS/i-ZnO/ZnO(Al) (d), SLG/Mo/CZTS/CdS/i-ZnO/ZnO(Al)/Al (e), CZTS thin-film solar cell (f).

The solar cell parameters of the CZTS thin-film solar cells which are V_{OC} , J_{SC} , FF, and solar cell efficiency were shown in **Figure 31**. From the results, it is evident that the solar cell performance was significantly improved by doping with Na. The average V_{OC} values of undoped CZTS, CZTS/15, and CZTS+5 were 120.6, 444.8, and 458.8 mV with a standard deviation of 89.8, 36.5, and 12.8 mV, respectively. The results show that V_{OC} significantly increase by doping with Na. It indicates that Na incorporation in CZTS thin-film helps increasing the p-type carrier concentration. Moreover, the betterment of film morphologies (e.g. uniformity and smooth surface) of Na-doped CZTS films which leads to lower recombination at the CZTS/CdS interface is one of the main reasons for higher V_{OC} .

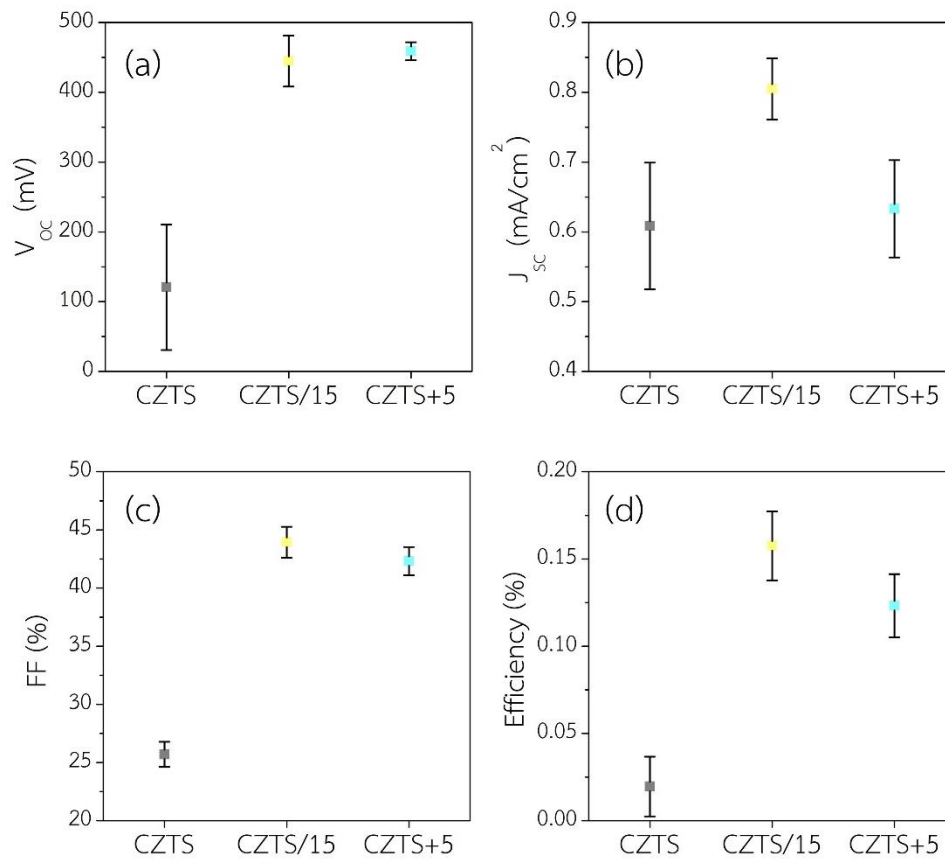


Figure 31: The plot of solar cell parameters of CZTS, CZTS/15, and CZTS+5.

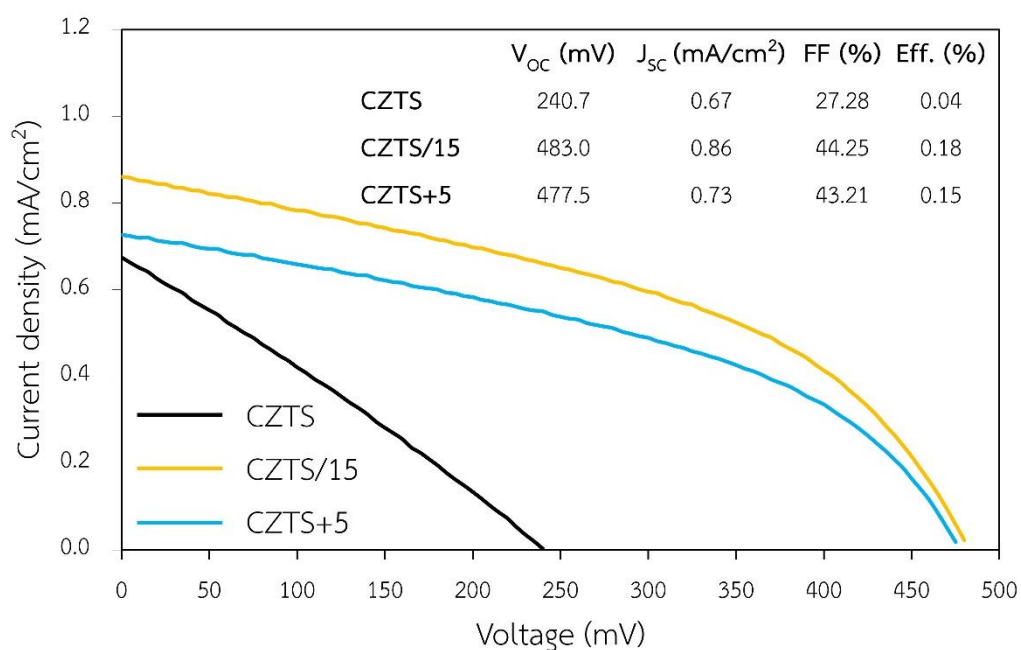
In addition, J_{SC} is increase by doping with Na. The average J_{SC} values of undoped CZTS, CZTS/15, and CZTS+5 were 0.61, 0.86, and 0.63 mA/cm² with a standard deviation of 0.09, 0.04, and 0.07 mA/cm², respectively. The improvement of J_{SC} is due to the improved CZTS crystallization which are beneficial for carrier transport as discussed in **Figure 26** (the cross-sectional images of the CZTS films). The higher V_{OC} and J_{SC} values of Na-doped CZTS solar cells were also related with the low series resistance (R_{Series}) and high shunt resistance (R_{Shunt}) which was summarized in **Table 7**. The undoped CZTS film has a shunt problem caused by pinholes, voids, and cracks in the CZTS layer lead to a significantly drop in V_{OC} and J_{SC} values.

Table 7: Characteristics parameters of CZTS, CZTS/15, and CZTS+5 solar cells*.

Samples	V_{OC} (mV)	J_{SC} (mA/cm ²)	FF (%)	R_{Series} (Ω cm ²)	R_{Shunt} (Ω cm ²)	Efficiency (%)
CZTS	240.7 (120.6)	0.67 (0.61)	27.28 (25.71)	39.55 (15.37)	283.9 (159.4)	0.04 (0.02)
CZTS/15	483.0 (444.8)	0.86 (0.80)	44.25 (43.94)	31.07 (10.87)	1979.0 (1626.5)	0.18 (0.16)
CZTS+5	477.5 (458.8)	0.73 (0.63)	43.21 (42.32)	5.28 (12.84)	1854.0 (1914.0)	0.15 (0.12)

* Values in parentheses are the average parameters of 4 devices.

The current density-voltage characterization of the best cell for undoped and Na-doped CZTS solar cells were shown in **Figure 32**.

**Figure 32:** The J-V curves of CZTS, CZTS/15, and CZTS+5 thin-film solar cells.

The highest V_{OC} and J_{SC} were obtained by doping with 15 mg/ml of NaCl solution on the CZTS thin-film. One of the reasons is because some Na⁺ ions from cations substitutions such as Na_{Cu} may be dissolved into water during CdS deposition.

The dissolving of Na^+ ions produce V_{Cu} on the CZTS surface. When the CdS layer is deposited by CBD method, Na^+ ions may occupy with Cd^+ ions resulting Cd_{Cu} defects which is beneficial for homogeneous p-n junction and carrier transportation [8]. Therefore, it can be concluded that Na-doping in CZTS thin-film by depositing the NaCl solution on the CZTS-thin-film is the best method in this experiment.

Improving V_{OC} and J_{SC} can improve FF directly and hence improves the solar cell efficiency. The average FF of undoped CZTS solar cell was 25.71 while the FF of CZTS/15 and CZTS+5 solar cells were increased to 43.94 and 42.32%, respectively. The highest efficiency of the undoped CZTS solar cell was 0.04% while the efficiency of CZTS/15 and CZTS+5 were increased to 0.18 and 0.15%, respectively. The undoped CZTS thin-film solar cell demonstrates the lowest performance due to the severe recombination of electron and hole at grain boundaries. The severe recombination is generated with pinholes, cracks, small grain size and rough surface of the CZTS absorber film as discussed in SEM and AFM results. Therefore, Na-doping in the CZTS absorber by both methods can improve the film morphologies and hence improves the solar cell performance. However, Na-doping in CZTS thin-film by depositing the NaCl solution on the CZTS-thin-film is better than the Na-doping by mixing NaCl in the CZTS solution. This is because Na^+ ions on the surface may be dissolved into water during CdS deposition resulting in a good formation of a p-n junction.

CHAPTER 5

CONCLUSIONS AND RECOMMENDATIONS

5.1 Conclusions

In this work, the CZTS thin-films were successfully synthesized using sol-gel convective deposition technique. The CZTS thin-film was doped with Na by depositing the NaCl solution on a CZTS thin-film and mixing NaCl in the CZTS solution in order to improve the film properties for use as an absorber layer in CZTS thin-film solar cell. The results found that Na-doping in the CZTS thin-films by both methods can improve the grain size, enhance film compactness, reduce the grain boundaries and surface roughness. The highest film quality is achieved by depositing 15 mg/ml of NaCl solution on the CZTS film and mixing 5% NaCl in CZTS solution. Moreover, the energy band gap of the CZTS films is in range of 1.5-1.6 eV which suitable for solar cell application.

Further investigation reveals that the V_{OC} , J_{SC} , and FF of Na-doping in CZTS thin-film solar cells were significantly improved, leading to better solar cell performance. The solar cell efficiency was increased from 0.04% to 0.18% by depositing 15 mg/ml of NaCl solution on the CZTS-thin-film. Na^+ ions on the surface from doping by depositing the NaCl solution on the CZTS-thin-film may be dissolved into water during CdS deposition resulting in a good formation of a p-n junction. Therefore, doping by depositing the NaCl solution on a CZTS thin-film is better than mixing NaCl in the CZTS solution.

5.2 Recommendations

The CZTS thin-films synthesized using sol-gel convective deposition technique in this experiment still have some drawbacks. It contains small grain and some pinholes in the films which lead to low solar cell performance. Thus, some process to synthesize the CZTS thin-films must be optimized in order to achieve higher film quality and solar cell efficiency.

1. Optimize the annealing process which are annealing temperature, annealing time, and ramp rate to find the optimum condition.
2. Optimize the thickness of the CZTS absorber layer in order to provide a good carrier transportation and achieve the higher current.
3. Optimize the Cu/(Zn+Sn) and Zn/Sn ratios in order to provide a good carrier transportation and achieve the higher current.
4. Optimize the concentration of CZTS solution in order to achieve higher growth rate of CZTS.



APPENDIX A

CALCULATION FOR CZTS SOL-GEL SOLUTION

The CZTS sol-gel solution was prepared using a concentration of Cu:Zn:Sn:S equal to 0.48:0.31:0.25:2 M. The calculation details for each chemical are shown belows:

Chemicals: $\text{CuCl}_2 \cdot 2\text{H}_2\text{O}$, Mw = 170.48 g/mol
 ZnCl_2 , Mw = 136.28 g/mol
 $\text{SnCl}_2 \cdot 2\text{H}_2\text{O}$, Mw = 225.63 g/mol
 $\text{SC}(\text{NH}_2)_2$, Mw = 76.12 g/mol

The amount of precursors solution is 20 ml.

$$\begin{aligned} \text{Amount of } \text{CuCl}_2 \cdot 2\text{H}_2\text{O} &= (0.48 \text{ mol/l}) \times (170.48 \text{ g/mol}) \times (0.02 \text{ l}) \\ &= 1.63 \text{ g} \end{aligned}$$

$$\begin{aligned} \text{Amount of } \text{ZnCl}_2 &= (0.31 \text{ mol/l}) \times (136.28 \text{ g/mol}) \times (0.02 \text{ l}) \\ &= 0.85 \text{ g} \end{aligned}$$

$$\begin{aligned} \text{Amount of } \text{SnCl}_2 \cdot 2\text{H}_2\text{O} &= (0.25 \text{ mol/l}) \times (225.63 \text{ g/mol}) \times (0.02 \text{ l}) \\ &= 1.13 \text{ g} \end{aligned}$$

$$\begin{aligned} \text{Amount of } \text{SC}(\text{NH}_2)_2 &= (2 \text{ mol/l}) \times (76.12 \text{ g/mol}) \times (0.02 \text{ l}) \\ &= 3.04 \text{ g} \end{aligned}$$

APPENDIX B

CALCULATION FOR SODIUM CONCENTRATION DEPOSITED ON THE CZTS
THIN-FILM

The concentrations of NaCl solution which were deposited on the CZTS thin-film was specified as 5, 10, and 15 mg/ml. The CZTS thin-film thickness is about 1.2 μm (deposited by convective deposition for 30 $\mu\text{l} \times 15$ times). The Na/(Cu+Zn+Sn) molar ratios of each film are shown below:

Example calculation for CZTS/5;

$$\frac{\text{Na}}{\text{Cu+Zn+Sn}} = \frac{\frac{5\text{mg}_{\text{NaCl}}}{\text{ml}} \times (30\mu\text{l} \times 15) \times \frac{\text{mol}}{58.44\text{g}_{\text{NaCl}}}}{\frac{0.038\text{g}_{\text{CuCl}_2 \cdot 2\text{H}_2\text{O}}}{170.48\text{g}_{\text{CuCl}_2 \cdot 2\text{H}_2\text{O}}/\text{mol}} + \frac{0.019\text{g}_{\text{ZnCl}_2}}{136.28\text{g}_{\text{ZnCl}_2}/\text{mol}} + \frac{0.0254\text{g}_{\text{SnCl}_2 \cdot 2\text{H}_2\text{O}}}{225.63\text{g}_{\text{SnCl}_2 \cdot 2\text{H}_2\text{O}}/\text{mol}}}$$

$$\frac{\text{Na}}{\text{Cu+Zn+Sn}} = \frac{0.026 \times 10^{-4} \text{ mol}}{(2.23 \times 10^{-4} \text{ mol}) + (1.39 \times 10^{-4} \text{ mol}) + (1.13 \times 10^{-4} \text{ mol})}$$

$$\frac{\text{Na}}{\text{Cu+Zn+Sn}} = 0.55\%$$

For CZTS/10;

$$\frac{\text{Na}}{\text{Cu+Zn+Sn}} = 1.07\%$$

For CZTS/15;

$$\frac{\text{Na}}{\text{Cu+Zn+Sn}} = 1.62\%$$

APPENDIX C

CALCULATION FOR SODIUM CONCENTRATION MIXED IN THE CZTS SOL-
GEL SOLUTION

The concentrations of NaCl solution which were mixed in the CZTS sol-gel solution was specified as 5%, 10%, and 15% mol NaCl to CZTS. The CZTS thin-film thickness is about 1.2 μm (deposited by convective deposition for 30 μl \times 15 times). The Na/(Cu+Zn+Sn) molar ratios of each film are shown below:

Example calculation for CZTS+5;

$$\frac{\text{Na}}{\text{Cu+Zn+Sn}} = \frac{\frac{0.0037\text{g}_{\text{NaCl}}}{58.44\text{g}_{\text{NaCl}}/\text{mol}}}{\frac{1.63\text{g}_{\text{CuCl}_2 \cdot 2\text{H}_2\text{O}}}{170.48\text{g}_{\text{CuCl}_2 \cdot 2\text{H}_2\text{O}}/\text{mol}} + \frac{0.85\text{g}_{\text{ZnCl}_2}}{136.28\text{g}_{\text{ZnCl}_2}/\text{mol}} + \frac{1.13\text{g}_{\text{SnCl}_2 \cdot 2\text{H}_2\text{O}}}{225.63\text{g}_{\text{SnCl}_2 \cdot 2\text{H}_2\text{O}}/\text{mol}}}$$

$$\frac{\text{Na}}{\text{Cu+Zn+Sn}} = \frac{0.063 \times 10^{-3} \text{mol}}{(9.56 \times 10^{-3} \text{mol}) + (6.24 \times 10^{-3} \text{mol}) + (5.01 \times 10^{-3} \text{mol})}$$

$$\frac{\text{Na}}{\text{Cu+Zn+Sn}} = 0.30\%$$

For CZTS+10;

$$\frac{\text{Na}}{\text{Cu+Zn+Sn}} = 0.60\%$$

For CZTS+15;

$$\frac{\text{Na}}{\text{Cu+Zn+Sn}} = 0.90\%$$

REFERENCES



จุฬาลงกรณ์มหาวิทยาลัย
CHULALONGKORN UNIVERSITY

1. Martin A. Green, Ewan D. Dunlop, Dean H. Levi, Jochen Hohl-Ebinger, Masahiro Yoshita, and Anita W.Y. Ho-Baillie, *Solar cell efficiency tables (version 54). Progress in Photovoltaics: Research and Applications*, 2019. **27**(7): p. 565-575.
2. Philip Jackson, Roland Wuerz, Dimitrios Hariskos, Erwin Lotter, Wolfram Witte, and Michael Powalla, *Effects of heavy alkali elements in Cu(In,Ga)Se₂ solar cells with efficiencies up to 22.6%*. *Physica status solidi (RRL) - Rapid Research Letters*, 2016. **10**(8): p. 583-586.
3. Siarhei Zhuk, Ajay Kushwaha, Terence K.S. Wong, Saeid Masudy-Panah, Aliaksandr Smirnov, and Goutam Kumar Dalapati, *Critical review on sputter-deposited Cu₂ZnSnS₄ (CZTS) based thin film photovoltaic technology focusing on device architecture and absorber quality on the solar cells performance*. *Solar Energy Materials and Solar Cells*, 2017. **171**: p. 239-252.
4. Ahmed Ziti, Bouchaib Hartiti, Hicham Labrim, Salah Fadili, Abderraouf Ridah, Bouchra Belhorma, Mounia Tahri, and Philippe Thevenin, *Study of kesterite CZTS thin films deposited by spin coating technique for photovoltaic applications*. *Superlattices and Microstructures*, 2019. **127**: p. 191-200.
5. G.L. Agawane, A.S. Kamble, S.A. Vanalakar, S.W. Shin, M.G. Gang, Jae Ho Yun, Jihye Gwak, A.V. Moholkar, and Jin Hyeok Kim, *Fabrication of 3.01% power conversion efficient high-quality CZTS thin film solar cells by a green and simple sol-gel technique*. *Materials Letters*, 2015. **158**: p. 58-61.
6. Wei Wang, Honglie Shen, Lydia Helena Wong, Zhenghua Su, Hanyu Yao, and Yufang Li, *A 4.92% efficiency Cu₂ZnSnS₄ solar cell from nanoparticle ink and molecular solution*. *RSC Advances*, 2016. **6**(59): p. 54049-54053.
7. Wei Wang, Honglie Shen, Lydia Helena Wong, Hanyu Yao, Zhenghua Su, and Yufang Li, *Preparation of high efficiency Cu₂ZnSn(S,Se)₄ solar cells from novel non-toxic hybrid ink*. *Journal of Power Sources*, 2016. **335**: p. 84-90.
8. Biwen Duan, Linbao Guo, Qing Yu, Jiangjian Shi, Huijue Wu, Yanhong Luo, Dongmei Li, Sixin Wu, Zhi Zheng, and Qingbo Meng, *Highly efficient solution-processed CZTSSe solar cells based on a convenient sodium-incorporated post-treatment method*. *Journal of Energy Chemistry*, 2020. **40**: p. 196-203.

9. Z. Laghfour, S. Aazou, M. Taibi, G. Schmerber, A. Ulyashin, A. Dinia, A. Slaoui, M. Abd-Lefdil, and Z. Sekkat, *Sodium doping mechanism on sol-gel processed kesterite Cu_2ZnSnS_4 thin films*. *Superlattices and Microstructures*, 2018. **120**: p. 747-752.
10. Peter T. Erslev, Jin Woo Lee, William N. Shafarman, and J. David Cohen, *The influence of Na on metastable defect kinetics in CIGS materials*. *Thin Solid Films*, 2009. **517**(7): p. 2277-2281.
11. M. Johnson, S. V. Baryshev, E. Thimsen, M. Manno, X. Zhang, I. V. Veryovkin, C. Leighton, and E. S. Aydil, *Alkali-metal-enhanced grain growth in Cu_2ZnSnS_4 thin films*. *Energy and Environmental Science*, 2014. **7**(6): p. 1931-1938.
12. Giovanni Altamura, Mingqing Wang, and Kwang-Leong Choy, *Influence of alkali metals (Na, Li, Rb) on the performance of electrostatic spray-assisted vapor deposited $Cu_2ZnSn(S,Se)_4$ solar cells*. *Scientific Reports*, 2016. **6**: p. 22109.
13. José Antonio Luceño-Sánchez, Ana María Díez-Pascual and Rafael Peña Capilla, *Materials for Photovoltaics: State of Art and Recent Developments*. *International Journal Molecular Sciences*, 2019. **20**(4): 976.
14. Kiran Ranabhat, Leev Patrikeev, Aleksandra Antal'evna Revina, Kirill Andrianov, Valerii Lapshinsky, and Elena Sofronova, *An introduction to solar cell technology*. Article in *Istrazivanja i projektovanja za privredu*, 2016. **14**(4): p. 481-491.
15. Tiantian Zhang, Meng Wang, and Hongxing Yang, *A Review of the Energy Performance and Life-Cycle Assessment of Building-Integrated Photovoltaic (BIPV) Systems*. *Energies*, 2018. **11**(11).
16. Jianhua Zhao, Aihua Wang, and Martin A.Green, *24.5% efficiency PERT silicon solar cells on SEH MCZ substrates and cell performance on other SEH CZ and FZ substrates*. *Solar Energy Materials and Solar Cells*, 2001. **66**: p. 27-36.
17. Andrew Blakers, Ngwe Zin, Keith R. McIntosh, and Kean Fong, *High Efficiency Silicon Solar Cells*. *Energy Procedia*, 2013. **33**: p. 1-10.
18. David D. Smith, Peter J. Cousins, Asnat Masad, Ann Waldhauer, Staffan Westerberg, Michael Johnson, Xiuwen Tu, Tim Dennis, Gabriel Harley, Genevieve Solomon, Seung Rim, Michael Shepherd, Scott Harrington, Michael Defensor, Arjelene Leygo, Princess Tomada, Junbo Wu, Thomas Pass, Laurice Ann Laurio Smith, Neil

- Bergstrom, Christopher Nicdao, Pauline Tipones, and Dennis Vicente, *Generation III High Efficiency Lower Cost Technology: Transition to full scale Manufacturing*. The 38th IEEE Photovoltaic Specialists Conference, Austin, Texas; 2012. p. 001594-001597.
19. Electricity Generation Authority of Thailand, *Silicon Solar cell technology*, Date viewed: Nov 1, 2019, Available from <http://www4.egat.co.th/re/solarcell/solarcell_technology.htm>
 20. V.V. Tyagi, Nurul A.A. Rahim, N.A. Rahim, and Jeyraj A./L. Selvaraj, *Progress in solar PV technology: Research and achievement*. Renewable and Sustainable Energy Reviews, 2013. **20**: p. 443-461.
 21. Images SI, Inc., *Photovoltaic Cells-Generating electricity*, Date viewed: Nov 2, 2019, Available from <<https://www.imagesco.com/articles/photovoltaic/photovoltaic-pg4.html>>
 22. Wenjie Li, Joel Ming Rui Tan, Shin Woei Leow, Stener Lie, Shlomo Magdassi, and Lydia Helena Wong, *Recent Progress in Solution-Processed Copper-Chalcogenide Thin-Film Solar Cells*. Energy Technology, 2018. **6**(1): p. 46-59.
 23. P. Prabeesh, I. Packia Selvam, and S. N. Potty, *Structural properties of CZTS thin films on glass and Mo coated glass substrates: a Rietveld refinement study*. Applied Physics A, 2018. **124**(3).
 24. Souad A. M. Al-Bat'hi, *Electrodeposition of Nanostructure Materials, Electroplating of Nanostructures*, IntechOpen; 2015.
 25. P. Avouris, B. Bhushan, D. Bimberg, K. von Klitzing, H. Sakaki, and R. Wiesendanger, *Nanostructured Materials and Their Applications*. NanoScience and Technology, Springer-Verlag Berlin Heidelberg; 2012.
 26. Wei Wang, Mark T. Winkler, Oki Gunawan, Tayfun Gokmen, Teodor K. Todorov, Yu Zhu, and David B. Mitzi, *Device Characteristics of CZTSSe Thin-Film Solar Cells with 12.6% Efficiency*. Advanced Energy Materials, 2014. **4**(7).
 27. Jeehwan Kim, Homare Hiroi, Teodor K Todorov, Oki Gunawan, Masaru Kuwahara, Tayfun Gokmen, Dhruv Nair, Marinus Hopstaken, Byungha Shin, Yun Seog Lee, Wei Wang, Hiroki Sugimoto, and David B Mitzi, *High efficiency*

- Cu₂ZnSn(S,Se)₄ solar cells by applying a double In₂S₃/CdS emitter.* *Advanced Materials*, 2014. 26(44): p. 7427-31.
28. Dattatray S. Dhawale, Adnan Ali, and Abhishek C. Lokhande, *Impact of various dopant elements on the properties of kesterite compounds for solar cell applications: a status review.* *Sustainable Energy & Fuels*, 2019. **3**(6): p. 1365-1383.
 29. Kaiwen Sun, Fangyang Liu, Chang Yan, Fangzhou Zhou, Jialiang Huang, Yansong Shen, Rong Liu, and Xiaojing Hao, *Influence of sodium incorporation on kesterite Cu₂ZnSnS₄ solar cells fabricated on stainless steel substrates.* *Solar Energy Materials and Solar Cells*, 2016. **157**: p. 565-571.
 30. Zhengfu Tong, Fangyang Liu, Liangxing Jiang, and Yanqing Lai, *Improving the crystallization and carrier recombination of Cu₂ZnSnS₄ thin film deposited on Mo-coated soda-lime glass by extra sodium doping through solution process.* *Materials Letters*, 2019. **254**: p. 50-53.
 31. Ionela Andreea Neacsu, Adrian Ionut Nicoara, Otilia Ruxandra Vasile and Bogdan Stefan Vasile, *Inorganic micro- and nanostructured implants for tissue engineering, Nanobiomaterials in Hard Tissue Engineering.* 2016. p. 271-295.
 32. Zhenghua Su, Kaiwen Sun, Zili Han, Hongtao Cui, Fangyang Liu, Yanqing Lai, Jie Li, Xiaojing Hao, Yexiang Liua, and Martin A. Green, *Fabrication of Cu₂ZnSnS₄ solar cells with 5.1% efficiency via thermal decomposition and reaction using a non-toxic sol-gel route.* *Journal of Materials Chemistry A*, 2014. **2**(2): p. 500-509.
 33. Laurell Technologies Corporation, *What is spin coating*, Date viewed: Nov 4, 2019, Available from < <http://www.spincoater.com/what-is-spin-coating.php>>
 34. Emma Spooner, *Large-Scale Deposition of Organic Solar Cells*, Ossila Ltd, Date viewed: Nov 4, 2019, Available from <<https://www.ossila.com/pages/opv-large-scale-deposition>>
 35. Napaporn Khothong, Thanawat Anantamongkolchai, and Paravee Vas-Umnuay, *Morphology and structure controlled fabrication of Cu₂ZnSnS₄ thin films by convective assembly deposition.* *Ceramics International*, 2019. **45**(5): p. 6102-6110.
 36. T. Chonsut, A. Rangkasikorn, S. Wirunchit, A. Kaewprajak, P. Kumnorkaew, N. Kayunkid, and J. Nukeaw, *Rapid convective deposition; an alternative method to*

- prepare organic thin film in scale of nanometer*. *Materials Today: Proceedings*, 2017. **4**(5): p. 6134-6139.
37. Kam Hoe Ong, Ramasamy Agileswari, Biancamaria Maniscalco, Panagiota Arnou, Chakrabarty Chandan Kumar, Jake W. Bowers, and Marayati Bte Marsadek, *Review on Substrate and Molybdenum Back Contact in CIGS Thin Film Solar Cell*. *International Journal of Photoenergy*, 2018. **2018**: p. 9106269.
 38. Syeda Adila Afghan, Husam Almusawi, and Husi Geza, *Simulating the electrical characteristics of a photovoltaic cell based on a single-diode equivalent circuit model*. *MATEC Web of Conferences*, 2017. **126**.
 39. Ling Yin, Guanming Cheng, Ye Feng, Zhaohui Li, Chunlei Yang, and Xudong Xiao, *Limitation factors for the performance of kesterite Cu_2ZnSnS_4 thin film solar cells studied by defect characterization*. *RSC Advances*, 2015. **5**(50): p. 40369-40374.
 40. Yanjie Wu, Yingrui Sui, Wenjie He, Fancong Zeng, Zhanwu Wang, Fengyou Wang, Bin Yao, and Lili Yang, *Substitution of Ag for Cu in $Cu_2ZnSn(S,Se)_4$: Toward Wide Band Gap Absorbers with Low Antisite Defects for Thin Film Solar Cells*. *Nanomaterials (Basel)*, 2020. **10**(1).
 41. Jie Zeng, Ke Liao, Zequn Chen, Yue Hu, Li Qin, Xiaoxin Li, Jianmei Xu, Ling Zhao, Wei Zhou, Qing Wang, and Jian Sun, *Na incorporation controlled single phase kesterite Cu_2ZnSnS_4 solar cell material*. *Materials Letters*, 2020. **265**.
 42. M. Marzougi, M. Ben Rabeh, and M. Kanzari, *Effect of Na doping on structural and optical properties in Cu_2ZnSnS_4 thin films synthesized by thermal evaporation method*. *Thin Solid Films*, 2019. **672**: p. 41-46.
 43. K.S. Gour, A.K. Yadav, O.P. Singh, and V.N. Singh, *Na incorporated improved properties of Cu_2ZnSnS_4 (CZTS) thin film by DC sputtering*. *Vacuum*, 2018. **154**: p. 148-153.

VITA

NAME Orawan Sukchoy

DATE OF BIRTH 14 March 1995

PLACE OF BIRTH Nakhon Si Thammarat, Thailand

INSTITUTIONS ATTENDED B.ing Petrochemical Engineering, Faculty of Engineering,
King Mongkut Institute of Technology Ladkrabang

HOME ADDRESS 11/56 Phraya Suren Road, Sam Wa Tawan Tok Subdistrict,
Khlomg Sam Wa District, Bangkok, Thailand, 10510

PUBLICATION Orawan Sukchoy, "Sodium Doping Effects on Properties of
CZTS Thin Films Fabricated by Sol-gel Convective
Deposition Technique", Proceeding of The Pure and
Applied Chemistry International Conference 2020
(PACCON 2020), Thailand